

---

# Understanding the Integration of Knowledge in Language Models with Graph Convolutions

---

Yifan Hou<sup>1</sup> Guoji Fu<sup>2</sup> Mrinmaya Sachan<sup>1</sup>

<sup>1</sup>Department of Computer Science, ETH Zürich <sup>2</sup>Southern University of Science and Technology  
{yifan.hou, mrinmaya.sachan}@inf.ethz.ch fugoji1995@outlook.com

## Abstract

Pretrained language models (LMs) do not capture factual knowledge very well. This has led to the development of a number of knowledge integration (KI) methods which aim to incorporate external knowledge into pretrained LMs. Even though KI methods show some performance gains over vanilla LMs, the inner-workings of these methods are not well-understood. For instance, it is unclear how and what kind of knowledge is effectively integrated into these models and if such integration may lead to catastrophic forgetting of already learned knowledge. This paper revisits the KI process in these models with an information-theoretic view and through a series of theoretical results, shows that KI can be interpreted using a graph convolution operation. With these results, we develop a probe model called *Graph Convolution Simulator* (GCS) for interpreting knowledge-enhanced LMs and exposing what kind of knowledge is integrated into these models. We conduct experiments to verify that our GCS can indeed be used to correctly interpret the KI process, and we use it to analyze two well-known knowledge-enhanced LMs: ERNIE and K-Adapter, and find that only a small amount of factual knowledge is integrated in them. We stratify knowledge in terms of various relation types and find that ERNIE and K-Adapter integrate different kinds of knowledge to different extent. Our analysis also shows that simply increasing the size of the KI corpus may not lead to better KI; fundamental advances are needed going forward.

## 1. Introduction

Pretrained language models (LMs) achieve impressive performance across various natural language processing (NLP) tasks. Previous works have shown that linguistic knowledge is captured quite well by LMs and it plays a vital role in their success (Liu et al., 2019a; Jawahar et al., 2019). How-

ever, factual knowledge is sparse and is expressed in varied ways in text. Thus, LMs are much worse in capturing factual knowledge about the world (Petroni et al., 2019; Wang et al., 2021b). This has led to the development of a variety of knowledge integration (KI) methods which aim to integrate external knowledge into LMs (Colon-Hernandez et al., 2021; Wang et al., 2021a; Zhang et al., 2019). Even though knowledge-enhanced LMs perform better on knowledge-intensive tasks, we lack a deep understanding about the inner workings of these models. Better downstream performance only indicates that some new knowledge has been integrated, but how much knowledge has been successfully integrated, and which type of knowledge is integrated in these models is still not well-understood.

To understand what knowledge is learned in LMs, many model-agnostic methods have been proposed. Previous works have proposed simple classifiers as probes (Ribeiro et al., 2016; Hewitt & Manning, 2019). To get more reliable interpretation, information-theoretic approaches have also been introduced (Guan et al., 2019; Pimentel et al., 2020; Hou & Sachan, 2021). Prompting is yet another way to understand what factual knowledge do these models learn. Prompts can be designed to let LMs solve text infilling problems, and the prompt performance can be interpreted as a probe (Petroni et al., 2019; Shin et al., 2020; Zhong et al., 2021). However, prompting relies on manually constructed templates which can be very time-consuming to construct. Factual knowledge is typically organized as large-scale sparse knowledge graphs (KGs). Previous interpretation methods such as linear probe are suitable for simple linguistic structures, but cannot provide reasonable interpretations for large sparse KGs.

There are two other common challenges in understanding KI. First, there are a large number of approaches for KI. KI in LMs can be implemented by matching sentences to entities or triples in knowledge graphs – called *entity-wise* integration (Peters et al., 2019; Zhang et al., 2019) and *triple-wise* integration (Liu et al., 2020; Wang et al., 2021a). There are several modeling choices (Colon-Hernandez et al., 2021) for KI, including modifications to the Transformer ar-

chitecture (Peters et al., 2019; Zhang et al., 2019; Liu et al., 2020), verbalizing knowledge triples and using data augmentation for finetuning (Agarwal et al., 2021), and designing objective functions that predict the factual knowledge (Yao et al., 2019; Wang et al., 2021a). How to design a general method to understand KI in all settings (e.g., entity-wise as well as triple-wise) is challenging. Furthermore, KI is typically implemented in a continual learning setup (Parisi et al., 2019) – KI is usually a secondary pretraining or finetuning step (Lu et al., 2021). As new knowledge is integrated, old knowledge could be *catastrophically forgotten* (CF; Kirkpatrick et al., 2016). KI could also lead to a situation called *catastrophic remembering* (CR; Kaushik et al., 2021), where the old knowledge may prevent the integration of new knowledge. Our understanding of these issues is limited.

In this paper, we first revisit the KI process (§2). We formulate KI with an information-theoretic view (§2.1), and construct a transformation to approximate the KI process (§2.2). Then, we prove that the KI process can be simulated by graph convolution operations (§2.3). Second, we introduce how to analyze KI, including the possibility of CR and CF. Specifically, we prove that the KI process can be interpreted by a graph attention mechanism (§3.1). Based on that, we propose a Graph Convolution Simulator (GCS) model to simulate and interpret the KI process (§3.2), and introduce the way to analyze its interpretation results (§3.3).

In our experiments, we verify that GCS can correctly interpret the KI process for two popular knowledge-enhanced LMs: ERNIE (Zhang et al., 2019) and K-Adapter (Wang et al., 2021a). We find that ERNIE is better at integrating entities with high degree in the KG, while K-Adapter integrates entities at leaf nodes in the KG well. We also find that CR often happens with popular entities (i.e. popular entities are harder to edit), while less popular entities are often catastrophically forgotten. In our qualitative study, we find that K-Adapter does not learn temporal knowledge at all. Finally, we investigate the correlation between the size of the KI corpus and KI quality, and find that there is no positive relationship between them. This suggests that merely building larger KI datasets may not be enough and we may need to make more fundamental advances to build better knowledge-enhanced LMs.

## 2. Simulating Knowledge Integration

In this section, we revisit KI with an information-theoretic lens, and prove that KI can be simulated by graph convolutions. We use MI to measure the knowledge learned in LMs, and use the change of MI to define KI, catastrophic remembering (CR), and catastrophic forgetting (CF). Then, we construct a multistep transformation to approximate the KI process. We show that KI can only happen in certain steps of the transformation, which are graph convolution

operations, leading to our final interpretation method, GCS.

### 2.1. Knowledge Integration Definition

Before presenting a formal definition of KI based on MI, we introduce some basic concepts. The notation used in this paper is summarized in Appendix A.

**Knowledge graphs.** We assume that factual knowledge can be formulated as a knowledge graph  $\mathcal{G} = (\mathcal{V}, \mathcal{E})$ , where nodes  $v_i \in \mathcal{V}$  represent entities, and edges in  $\mathcal{E}$  represent relations between them. Let  $\mathcal{N}_{v_i}$  denote the set of neighbors of node  $v_i$ , and  $t_i$  denote the entity label corresponding to the node  $v_i$ . Further, let  $\mathbf{x}_i = \text{LM}(t_i)$  denote the entity (label) representations of  $t_i$  given by a LM<sup>1</sup>. Let  $\mathbf{X} \in \mathbb{R}^{|\mathcal{V}| \times d}$  denote a matrix formed by stacking all entity representations  $\mathbf{x}_i \in \mathbb{R}^d$ . In this paper, we only consider nodes and edges in the KG and ignore other kinds of information such as edge weights, edge directions and multi-edges (multi-relations).

**Information-theoretic probe.** We follow the theoretical setting of Hou & Sachan (2021) that measures the knowledge captured in LMs by MI. We assume that the local graph  $\mathcal{G}(v_i)$  contains all the factual information regarding  $v_i$ . In this work, we consider factual knowledge in the form of triples  $(v_i, r, v_j)$ . Since a triple only contains entities within one-hop, it suffices to set  $\mathcal{G}(v_i) = \mathcal{N}_{v_i}$  the one-hop neighborhood of  $v_i$ . Factual knowledge that has been successfully integrated should be reflected in entity representations. Let  $\mathbf{x}$  be a random variable that takes values ranging over all possible entity representations of a LM<sup>2</sup>, and  $\mathbf{g}$  be a random variable that ranges over all possible corresponding local structures  $\mathcal{G}(v_i)$ . Intuitively,  $\text{MI}(\mathbf{x}; \mathbf{g})$  measures the amount of information in  $\mathbf{g}$  that is contained in  $\mathbf{x}$ .

**Definition 2.1** (Knowledge Integration). Given  $\mathcal{G}$ , let entity representation matrices given by a LM before and after KI be  $\mathbf{X}$  and  $\mathbf{H}$ . Their corresponding random variables are  $\mathbf{g}$ ,  $\mathbf{x}$ , and  $\mathbf{h}$ . We formulate KI process  $f(\mathbf{x}, \mathbf{g}) = \mathbf{h}$  as the change of MI:  $\text{MI}(\mathbf{x}; \mathbf{g}) \rightarrow \text{MI}(\mathbf{h}; \mathbf{g})$ , i.e., knowledge of  $\mathbf{g}$  is integrated into  $\mathbf{x}$  to get  $\mathbf{h}$ . If  $\text{MI}(\mathbf{h}; \mathbf{g}) \approx \text{MI}(\mathbf{x}; \mathbf{g})$ , it means that CR happens, i.e., there is a failure to integrate new knowledge. If CF happens, we have  $\text{MI}(\mathbf{h}; \mathbf{x}) \approx 0$ .

The definition can be intuitively visualized by Figure 1. The MI change can be represented by regions 1 and 4 in the Venn diagram. Ideally, if we have  $\text{MI}(\mathbf{h}; \mathbf{g}) - \text{MI}(\mathbf{x}; \mathbf{g}) \approx \text{MI}(\mathbf{g}; \mathbf{g}) -$

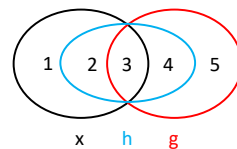


**Figure 1:** Venn diagram for MI visualization.  $\mathbf{x}$ ,  $\mathbf{h}$ , and  $\mathbf{g}$  are random variables.

<sup>1</sup>We represent each entity as the average of its word(-piece) embeddings given by the LM as Hewitt & Manning (2019) and Hou & Sachan (2021).

<sup>2</sup>Here, the set of entity representations  $\mathbf{X} \in \mathbb{R}^{|\mathcal{V}| \times d}$  can be regarded as empirical samples from  $\mathbf{x}$ .

$MI(\mathbf{x}; \mathbf{g})$ , i.e., the region 5 is small, we say most knowledge is successfully integrated. If little new knowledge has been integrated, region 4 is very small. Then, we say that CR has happened. If CF happens, most knowledge in  $\mathbf{x}$  is forgotten in  $\mathbf{h}$  after KI, and region 1 is large. Successful KI happens when much new knowledge is integrated (i.e.,  $MI(\mathbf{h}; \mathbf{g})$  is large) and little old knowledge is forgotten (i.e.,  $MI(\mathbf{h}; \mathbf{x})$  is large).

## 2.2. Constructing an Approximate Transformation

In this subsection, we show that we can construct a transformation to approximate the KI process with arbitrary accuracy. We begin by introducing the concept of Graph Fourier transforms.

**Graph Fourier transformation.** Graph Fourier transform (GFT) can be used to transform the entity representation matrix  $\mathbf{X}$  in the Euclidean space to the graph spectral domain (i.e., KG space). Specifically, let  $\mathbf{A} \in \mathbb{R}^{|\mathcal{V}| \times |\mathcal{V}|}$  be the symmetric adjacency matrix corresponding to  $\mathcal{G}$ . Let  $\mathbf{L}_n = \mathbf{I} - \mathbf{D}^{-1/2} \mathbf{A} \mathbf{D}^{-1/2}$  denote the normalized Laplacian matrix for  $\mathcal{G}$ , where  $\mathbf{D}$  denotes the degree matrix. We do the eigendecomposition for  $\mathbf{L}_n$  as  $\mathbf{L}_n = \mathbf{U} \mathbf{\Lambda} \mathbf{U}^T$ , where  $\mathbf{U}$  is the matrix of eigenvectors ordered by eigenvalues and  $\mathbf{\Lambda} = \text{diag}(\lambda_1, \lambda_2, \dots, \lambda_N)$  is the diagonal matrix of eigenvalues. Based on the GFT (Sandryhaila & Moura, 2014), formally, the transformation of  $\mathbf{X}$  to the KG space can be written as  $\text{GFT}(\mathbf{X}) = \mathbf{U}^T \mathbf{X}$ , and its inverse transformation can be written as  $\text{RGFT}(\text{GFT}(\mathbf{X})) = \mathbf{U} \text{GFT}(\mathbf{X}) = \mathbf{X}$ .

It is intractable to directly simulate the KI process (i.e., integration of information from  $\mathbf{g}$  into  $\mathbf{x}$  to get  $\mathbf{h}$  (Definition 2.1)) with simple probe models since  $\mathbf{g}$  is graph data that is not in the Euclidean space. Fortunately, with GFT, we can transform  $\mathbf{x}$  and  $\mathbf{h}$  into the KG space, and design a probe in that space to simulate the KI process. The theorem below provides a way to construct a probe that can simulate the KI process with arbitrary accuracy.

**Theorem 2.2** (Transformation Existence). *Denote the graph Fourier transformation and its inverse transformation in terms of  $\mathcal{G}$  as  $\text{GFT}(\cdot)$  and  $\text{RGFT}(\cdot)$ . Given a LM and its knowledge-enhanced version, suppose that  $MI(\mathbf{x}; \mathbf{g}) < MI(\mathbf{h}; \mathbf{g})$ , there exists a mapping that satisfies  $f(\mathbf{x}, \mathbf{g}) = \mathbf{h}$ . Then, for any  $\epsilon > 0$ , there exists a neural network  $\text{NN}(\cdot)$  such that*

$$|f(\mathbf{x}, \mathbf{g}) - \text{RGFT}(\text{NN}(\text{GFT}(\mathbf{x})))| < \epsilon. \quad (1)$$

The proof can be found in Appendix B. Theorem 2.2 shows that there exists an approximate transformation composed of GFT and a neural network that can simulate the KI process (i.e.,  $f(\mathbf{x}, \mathbf{g}) = \mathbf{h}$ ) with arbitrary accuracy. In practice, the mapping  $f(\mathbf{x}, \mathbf{g})$  is realized by complex KI training process on large LMs with new datasets, objectives, or even

new LM parameters. Here, we can use a simple transformation  $\text{RGFT}(\text{NN}(\text{GFT}(\mathbf{x})))$  to generally approximate and simulate the complex KI process. However, there is a challenge. KGs are normally very large, and computing the eigendecomposition of the Laplacian matrix for GFT is prohibitively expensive. Besides, the transformation is not interpretable, so it cannot be used as a probe model directly. Thus, we take a deeper look into this transformation and show that it can be further simplified into a set of graph convolutions.

## 2.3. KI Simulation with Graph Convolutions

In this subsection, we introduce details of the transformation in Theorem 2.2. We prove that even if there are multiple steps of the transformation, MI change only happens in certain steps. We show that these steps are equivalent to graph convolutions.

**Graph convolutions.** Convolution operations on graphs are often used to model the relational information of KGs, where entities aggregate information from their neighbors and pass the information along based on the graph structure. Graph convolutions can be implemented by filters (i.e., kernels)  $g_\Theta$  in the graph spectral domain (i.e., KG space). As the GFT of the convolution of  $g_\Theta$  and  $\mathbf{X}$  is the pointwise product of their GFT (Bracewell & Bracewell, 1986), the convolution can be written as  $g_\Theta \star \mathbf{X} = \text{RGFT}(g_\Theta \cdot \text{GFT}(\mathbf{X}))$  (Bruna et al., 2014).

In the below proposition, we show that the multistep transformation for KI simulation (Theorem 2) can be simplified as graph convolutions.

**Proposition 2.3** (Graph Convolutions for Simulation). *Suppose  $MI(\mathbf{x}; \mathbf{g}) < MI(\mathbf{h}; \mathbf{g})$ ,  $MI(\mathbf{h}; \mathbf{x}) < MI(\mathbf{x}; \mathbf{x})$ . The mapping  $f(\mathbf{x}, \mathbf{g}) = \mathbf{h}$  can be approximated by the transformation  $\text{RGFT}(\text{NN}(\text{GFT}(\mathbf{x})))$  where  $\text{NN}(\cdot)$  has  $n$  layers. Furthermore, we can use  $n$  linear functions (i.e., graph convolutions) in  $\text{NN}(\cdot)$  to simulate the MI change well.*

Proposition 2.3 indicates that we can simply use  $n$  linear functions instead of the whole transformation in Theorem 2.2 to simulate the MI change (i.e., the KI process). These linear functions in the KG space are actually graph convolution operations. And thus, we can circumvent the expensive eigen-decomposition in GFT with fast and well-approximated graph filters (Defferrard et al., 2016; Kipf & Welling, 2017). The formal proof is in Appendix C. Figure 2 briefly illustrates the overall idea.

The shown black dashed transformation proposed in Theorem 2.2 can simulate KI with arbitrary accuracy. Even though the transformation is simple, it is not very efficient with large KGs and not interpretable. The solid red lines represent the simulation of KI using graph convolutions (Proposition 2.3), which are much more fast and could be

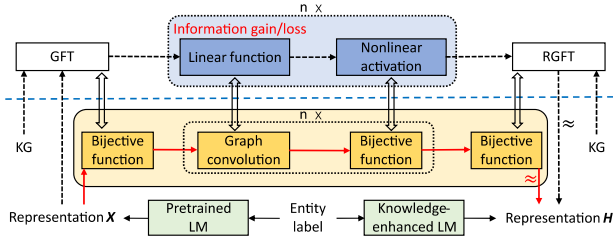


**Figure 2:** Illustration of the KI simulation. The part above the horizontal blue dashed line represents graph spectral domain (i.e., KG space). Black dashed arrows show the approximated transformation in Theorem 2.2. Red arrows show the simplified simulation with graph convolutions in Proposition 2.3.

interpretable.

According to the invariance property of MI (Kraskov et al., 2004), the introduction of bijective functions does not introduce any new information – MI remains unchanged upon the introduction of bijective functions. We know that GFT and RGFT are both bijective (Appendix C.1). We show that nonlinear activation functions in a neural network (e.g.,  $\text{sigmoid}(\cdot)$ ) are bijective as well (Appendix C.1). Thus, the MI change in the KI process can only happen in the linear function (Appendix C.2). Based on the convolution theorem (Bracewell & Bracewell, 1986), linear functions in graph space are graph convolutions (Sandryhaila & Moura, 2014; Bruna et al., 2014; Kipf & Welling, 2017) (Appendix C.3). Thus, we can simply use graph convolution operations instead to simulate the KI process.

### 3. Interpreting Knowledge Integration

In the last section, we showed that KI can be simulated by graph convolutions. In this section, we introduce the mechanism to interpret the KI process. Specifically, we first illustrate that the graph attention mechanism can be used to interpret graph convolutions. Then, we introduce an implementation of the probe model proposed in our work: Graph Convolution Simulator (GCS), as well as a method to analyze our interpretation results.

#### 3.1. Knowledge Integration with Graph Attention

Following Proposition 2.3, we can select powerful graph filters to simulate and interpret the KI process. Velickovic et al. (2018) and Thekumparampil et al. (2018) introduce the attention mechanism to graph filters, where the contribution of each edge to the convolution can be shown explicitly. Graph attention makes filters more powerful and convolutions more interpretable (Fu et al., 2020).

**Proposition 3.1** (Graph Attention for Interpretation). *Suppose  $\text{MI}(\mathbf{x}; \mathbf{g}) < \text{MI}(\mathbf{h}; \mathbf{g})$ ,  $\text{MI}(\mathbf{h}; \mathbf{x}) < \text{MI}(\mathbf{x}; \mathbf{x})$ , and the KI process  $\text{MI}(\mathbf{x}; \mathbf{g}) \rightarrow \text{MI}(\mathbf{h}; \mathbf{g})$  can be simulated well by  $n$  graph convolution operations. Then, we can use the attention coefficients on edges and self-loops to interpret*

*the KI, including CR and CF.*

The formal proof can be found in Appendix D. Note that we have  $n$  graph convolutions, and they function differently (Bruna et al., 2014). In a multi-layer graph convolution network, the  $k$ -th graph convolution step aggregates information from  $k$ -hop neighbors<sup>3</sup>. In this work, we consider integration of knowledge in the form of knowledge triples. Knowledge triples link entities within 1-hop. Thus, in practice, we set  $n = 1$  for simplicity in our work. According to Fu et al. (2020), graph attention can also be seen as edge denoising. This provides an alternative explanation of our GCS probe from the denoising view. More details can be found in Appendix D.

#### 3.2. GCS architecture.

Based on Proposition 2.3 and Proposition 3.1, we design GCS with two bijective functions and one graph convolution function in between. To implement a bijective function in practice, we show that special MLP layers can be bijective if the weight matrix is a square matrix (plus a small noise). The formal description and the proof are in Appendix E. We design our GCS model with one graph convolutional layer and two bijective MLP layers as:

$$\text{GCS}_{\theta_1}(\cdot) = \text{MLP}_n(\text{GC}(\text{MLP}_n(\cdot), \mathcal{G})), \quad (2)$$

where  $\text{MLP}_n(\cdot)$  is the bijective MLP layer and  $\text{GC}(\cdot, \mathcal{G})$  is the graph convolutional layer on the KG  $\mathcal{G}$  which is used to simulate and interpret the KI process. Given an entity  $v_i$  and its set of neighbors  $\mathcal{N}_{v_i}$ , we can write the graph convolutional layer as:

$$\text{GC}(\mathbf{x}_i) = \sigma \left( \sum_{v_j \in \mathcal{N}_{v_i} \cup \{v_i\}} a_{i,j} \mathbf{W}^V \mathbf{x}_j \right), \quad (3)$$

$$a_{i,j} = \text{softmax} \left( \frac{(\mathbf{W}^Q \mathbf{x}_i) \cdot (\mathbf{W}^K \mathbf{x}_j)}{\sqrt{d_k \cdot t}} \right).$$

Here,  $\mathbf{x}_i$  is the entity representation of  $v_i$  before knowledge integration, the activation function  $\sigma(\cdot)$  is  $\text{ELU}(\cdot)$ , and  $\mathbf{W}^V$  is a weight matrix.  $a_{i,j}$  is the attention coefficient on the relation that connects  $v_i$  and  $v_j$ .  $\mathbf{W}^Q$  and  $\mathbf{W}^K$  are two parameter matrices in the graph attention.  $d_k$  is the dimension of vector  $\mathbf{W}^K \mathbf{x}_j$ , and  $\text{softmax}(\cdot)$  is the edge-wise softmax function with respect to node  $v_i$ . Temperature  $t$  is a hyperparameter that controls the attention distribution to be hard or soft. As the multiplicative attention mechanism (Vaswani et al., 2017) is broadly used in LMs, we also select multiplicative attention in the graph attention. We optimize GCS by letting its outputs be close to  $\mathbf{h}$  as Equation 4.

$$\mathcal{L} = -\text{MI}(\text{GCS}_{\theta_1}(\mathbf{x}); \mathbf{h}). \quad (4)$$

<sup>3</sup>Note that the number of graph convolutional layers decides the receptive field of entities.  $n$  layers represent that each entity can get information from its  $n$ -hop neighbors.

We use the MI maximization as the objective. In practice, we maximize the compression lemma lower bound (Belghazi et al., 2018). Details are in Appendix F.3.

### 3.3. Analyzing Interpretation Results In Practice

Figure 3 gives an example of interpreting KI by GCS. We first encode entity labels with the LMs and get entity representations. After KI, the entity representation of knowledge-enhanced LM become different. Then, we implement GCS as equation 2, optimize it using equation 4 and use its attention coefficients (equation 3) to interpret KI. From the results given by GCS (KG at the bottom), we find that entity “Da Vinci” focuses more on entity “Mona Lisa”. This implies that “(Da Vinci, painted, Mona Lisa)” is integrated, while another triple is not. Below we discuss how to use attention coefficients to interpret CR and CF.

As introduced in §3.1, large edge attention coefficients mean that the triples corresponding to the relation are integrated well. To understand CR and CF, we add self-loops on entities in the KG, and use attention coefficients on the self-loops to show how much of the original information is remembered/forgotten for entities. In particular, large self-loop attention coefficients mean that the original entity information is kept well. Thus, we introduce thresholds to analyze our interpretation results as follows<sup>4</sup>. We simply regard triples with  $a_{i,j} > 0.1$  on edges as learned triples. Entities with  $a_{i,i} < 0.1$  on self-loops means CF has happened, where much new factual knowledge information is integrated and original entity information is forgotten. Correspondingly,  $a_{i,i} > 0.9$  means CR has happened. For the example in Figure 3, we can find that CR happens to entity “Person”, and CF happens to entity “Da Vinci”.

## 4. Experiments

We begin this section by introducing two knowledge-enhanced LMs considered in this work: ERNIE (Zhang et al., 2019) and K-Adapter (Wang et al., 2021a). Knowl-

<sup>4</sup>Note that users may choose different thresholds. We heuristically set these thresholds for our analysis.

edge is integrated in an entity-wise manner in ERNIE, and a triple-wise manner in K-Adapter (described in §4.1). Then, we move on to our experiments. First, we verify our GCS model from three different aspects (§4.2). We prove that GCS can correctly interpret how much KG information is integrated, as well as which set of entities and triples are integrated. Second, we use GCS to interpret the KI process for ERNIE and K-Adapter (§4.3). We present the interpretation results and find that both of them have only integrated few triples but many entities. Besides, we analyze the interpretation results to understand which kinds of knowledge is integrated well in these models. In order to do this, we stratify knowledge in terms of various relation types and find that ERNIE and K-Adapter integrate different kinds of factual knowledge to different extent. Finally, we analyze the correlation between the size of KI corpus and KI quality, and find that there is no positive relationship between them.

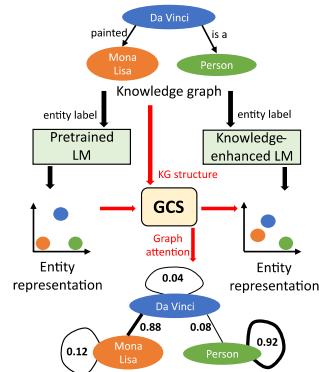


**Figure 3:** An example of interpreting KI by GCS. Black arrows show the procedure to get entity representations, and red arrows show how to use GCS to interpret KI. Attention weights (denoted by thickness of the edges) give us the final interpretation.

### 4.1. Knowledge-Enhanced Models

**ERNIE.** ERNIE integrates factual knowledge into BERT (Devlin et al., 2019) directly without introducing extra parameters. The Wikipedia corpus and Wikidata knowledge triples are selected for integration. As there is no provided alignment between natural sentences and knowledge entities, ERNIE uses TAGME (Ferragina & Scaiella, 2010) to extract entity mentions in sentences and aligns them with corresponding entities in KGs. A new objective is designed for KI in addition to the standard MLM and NSP objectives: alignments in the input text are randomly masked, and the model is asked to select aligned entities from KGs. Different from K-Adapter that stores factual knowledge in newly introduced parameters, when ERNIE finds the aligned entity, its embedding obtained from Bordes et al. (2013) is integrated into the output representations. Thus, during inference, the KG and its embeddings are still required to be fed into ERNIE.

**K-Adapter.** K-Adapter takes RoBERTa (Liu et al., 2019b) as the backbone model and inserts three new layers into RoBERTa to learn new knowledge. The final output is concatenated with the output of RoBERTa<sup>5</sup>. During the integration, parameters of RoBERTa are frozen, only parameters of the newly inserted layers are updated. K-Adapter uses the T-REx-rc (EISahar et al., 2018) dataset for KI, which has an alignment of natural sentences with knowledge triples in Wikidata. For the KI objective, K-Adapter decides whether certain relations exist or not, and classifies relation labels given the aligned sentence. As knowledge is integrated in newly inserted layers, the model no longer needs to use the T-REx-rc dataset for inference, and it can be finetuned like any other pretrained LMs on downstream tasks.

<sup>5</sup>Note that here we only consider factual knowledge, thus, the linguistic Adapter is not used.

## 4.2. GCS Verification

We design a set of experiments to verify that GCS can indeed correctly interpret the KI process. We first verify that GCS can correctly interpret how much knowledge is integrated using synthetic experiments (§4.2.1). Then, we verify that GCS can correctly interpret which type of knowledge is integrated based on a KI dataset (§4.2.2) and downstream task performance (§4.2.3).

### 4.2.1. SYNTHETIC EXPERIMENT

In our first experiment, we simulate synthetic KI processes where different amounts of knowledge is integrated into a LM, and test whether GCS can interpret them correctly.

**Setting.** We use DeepWalk (Perozzi et al., 2014) to obtain entity embeddings (i.e., KG embeddings) of the KG that is used for KI. We regard the obtained KG embeddings as the entity representations of knowledge-enhanced LMs, and we add Gaussian noise with different noise ratios on the KG embeddings and regard the noisy representations as the entity representations of vanilla LMs. The KG embeddings can be regarded as entity representations that contain almost all (e.g., 100%) information of the KG, and noisy KG embedding contain some (e.g., 50%) information of the KG. As noise ratio increases, it means that more knowledge is integrated into the LM during the synthetic KI process. The synthetic KI process thus can be regarded as integrating factual knowledge to a varying degree (from 50% to 100%). Then, we use GCS to interpret synthetic KI processes from vanilla LMs to knowledge-enhanced LMs.

**Results.** Figure 11 shows the results. We use the mean value of self-loop attention coefficients to show how much knowledge is integrated: large values mean that little knowledge is integrated. For the convenience of observation, we report one minus the mean value in Figure 4. We observe the tendency of the red curve which shows interpretation results for the synthetic KI processes. When the noise ratio increases, GCS can correctly interpret that more information is integrated. When we combine the practical interpretation results for ERNIE and K-Adapter and use the results of our synthetic experiment as reference, we can find that both of these models integrate some but not all factual knowledge (precisely 24% for ERNIE and 31% for K-Adapter).

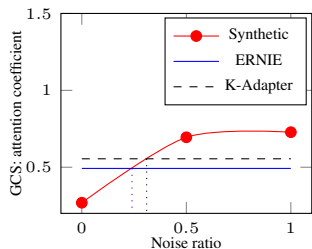


**Figure 4:** Interpretation results of how much knowledge is integrated in synthetic KI processes. The red curve shows the interpretation results for our probe on synthetic KI processes. Blue solid lines and black dashed lines are the KI interpretation results for ERNIE and K-Adapter in practice.

We also implemented three classic probe methods as baselines for comparison (see Appendix H.1). However, we found that these probes cannot correctly show how much knowledge is integrated. Only GCS can provide reasonable results for ERNIE and K-Adapter. In contrast, the interpretation results given by other probe baselines show that ERNIE and K-Adapter do not integrate any factual knowledge or some factual knowledge is even forgotten after integration. Besides, in Appendix H.2, we discuss that the linear probe (i.e., linear classifier) is not suitable for KI interpretation since its bias and variance are large.

### 4.2.2. VERIFICATION VIA THE KI CORPUS

As our second verification experiment, we only use the factual knowledge that is identified as learned by GCS to enhance BERT and RoBERTa to get ERNIE (drop-UE) and K-Adapter (drop-UE), and then test them on two downstream tasks. If GCS correctly interpreted the KI process, the performance of the drop-UE versions should be roughly the same as that of ERNIE/K-Adapter.

**Setting.** This experiment is composed of three steps. First, we use GCS to interpret the KI process in ERNIE and K-Adapter, and identify triples or entities that are integrated successfully. Second, we re-enhance BERT/RoBERTa to get ERNIE (drop-UE) / K-Adapter (drop-UE) only using the entities/triples that are identified as successfully integrated. Third, we finetune ERNIE/K-Adapter and their drop-UE versions on two downstream tasks.

As introduced in §4.1, ERNIE and K-Adapter integrate knowledge by using aligned natural sentences instead of using entities/triples directly. Thus, after we get the interpretation results, i.e., entities with self-loop attention coefficients smaller than 0.9 or triples with edge attention coefficients larger than 0.1, we only keep KI corpus aligned with the integrated knowledge. Specifically, we only keep 61.72% entity embeddings (obtained by Bordes et al. (2013)) for ERNIE (drop-UE), and 10.09% KI corpus (i.e., natural sentences) that aligned with successfully integrated triples for K-Adapter (drop-UE). Detailed statistics are in Appendix G. Then, we finetune them on two downstream tasks (entity typing) that ERNIE and K-Adapter outperform BERT and RoBERTa most significantly on: OpenEntity (Choi et al., 2018) and FIGER (Ling et al., 2015). Implementation details of ERNIE, K-Adapter, and GCS can be found in Appendix F.2 and Appendix F.3.

**Table 1:** Performance of ERNIE, K-Adapter and their drop-UE versions on entity typing on the OpenEntity and FIGER datasets.

Model	OpenEntity			FIGER		
	P	R	F1-Micro	P	R	F1-Micro
ERNIE	78.24	68.75	73.19	77.39	65.81	71.13
ERNIE (drop-UE)	78.11	71.43	74.62 ↑	77.38	64.90	70.60 ↓
K-Adapter	76.63	75.26	75.94	67.50	88.79	76.69
K-Adapter (drop-UE)	75.95	75.95	75.95 ↑	67.29	88.88	76.59 ↓

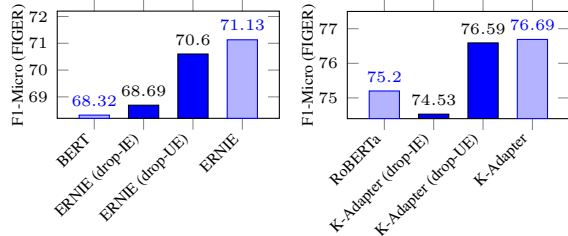


**Figure 5:** Performance of BERT, RoBERTa, ERNIE, K-Adapter, and their KI corpus dropped versions on the FIGER dataset.

**Results.** From Table 1, we find that even if we drop large amount of KI data in this way, the performance of drop-UE versions on entity typing task is roughly the same as original (reproduced) versions. For the OpenEntity dataset, better performance is even achieved. Regarding the FIGER dataset, the performance of drop-UE versions is slightly worse. We also report the performance of BERT, RoBERTa, and two drop-IE<sup>6</sup> versions in Figure 5. We find that compared to dropping KI corpus aligned with integrated knowledge, dropping KI corpus aligned with non-integrated knowledge achieves much better performance. Thus, we verify that GCS can provide correct interpretation results.

#### 4.2.3. VERIFICATION VIA A DOWNSTREAM TASK

We use the performance of ERNIE and K-Adapter on the test set of downstream tasks to verify that GCS provides correct interpretation results. If GCS correctly interpreted the KI process, knowledge-enhanced LMs should perform better on the test set without samples aligned with non-integrated knowledge and vice versa.

**Settings.** We first align entities in the KI corpus and the OpenEntity dataset based on their *Wikidata Q identifier*<sup>7</sup>. For the entity typing task (OpenEntity dataset), we drop samples in the finetuning test set that aligns with the integrated knowledge and non-integrated entities (called *w/o-IE* test set and *w/o-UE* test set), and test ERNIE and K-Adapter on the two dropped test sets. Detailed statistics can be found in the Table 7 in Appendix G.

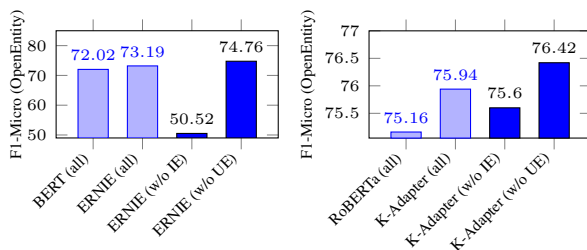


**Figure 6:** Performance of BERT, RoBERTa, ERNIE, K-Adapter on the OpenEntity dataset for different test sets (original versions and dropped versions).

<sup>6</sup>The drop-IE versions mean that we drop KI corpus aligned with integrated factual knowledge identified by GCS and use the corpus to enhance BERT and RoBERTa.

<sup>7</sup><https://www.wikidata.org/wiki/Q43649390>

**Results.** Figure 6 shows the results. We can find that for ERNIE, the changes are significant. The performance (F1-Micro) on the test set (w/o-IE) is more than 20 F1 points worse than that on the complete test set (all). And for K-Adapter, there is a drop in F1 on the w/o-IE set and increase in F1 on the w/o-UE set (albeit small). We hypothesize that this may be because of the differences in the finetuning objective and the KI objective<sup>8</sup>, and because the knowledge integrated in K-Adapter may change during finetuning. These results verify that GCS can correctly interpret which set of knowledge is integrated.

### 4.3. GCS Findings

After verifying GCS with three groups of experiments, we analyze the interpretation results. We find that both ERNIE and K-Adapter integrate many knowledge entities ( $\approx 60\% - 70\%$ ) but only few knowledge triples ( $\approx 20\% - 30\%$ ). Detailed results can be found in Figure 8 in Appendix G. Next, we classify knowledge based on the relation types (in terms of their topology type and Wiki data type) and analyze how ERNIE and K-Adapter integrate knowledge with certain relation types.

#### 4.3.1. ANALYSIS VIA RELATION TOPOLOGY

We classify relations into three types based on their topology features, since entities in the complex structure (i.e., connected to many other entities) tend to be common. Following previous work (Bordes et al., 2013; Tang et al., 2020), we denote relations that connect two leaf nodes (entities) in the KG as  $1 - 1$  relations, and relations that connect two center nodes (entities) in the KG as  $N - M$  relations. Other relations are denoted as  $N - 1$  relations. An example is in Figure 9 in Appendix G. We perform an analysis in terms of different types of relations and report the percentage of successfully integrated entities and triples for ERNIE and K-Adapter for each relation type. For each relation type, we also present the percentage of connected entities that are catastrophically remembered or forgotten (CR and CF).

Figure 7 presents specific results, and detailed statistics can be found in Table 8 in Appendix G. We find that for ERNIE, entities connected with  $1 - 1$  and  $N - M$  relations are captured well. But entities connected to  $N - 1$  relations are not. Since ERNIE relies on KG embedding to learn structure knowledge, KI is highly consistent with the quality of the KG embedding provided in Bordes et al. (2013).

K-Adapter shows different behaviors. Triples with  $N - M$  relations are not captured well. However, K-Adapter integrates triples with  $1 - 1$  relations well. This phenomenon is common for Transformer encoders, where knowledge

<sup>8</sup>K-Adapter integrates knowledge in a triple-wise manner instead of entity-wise.

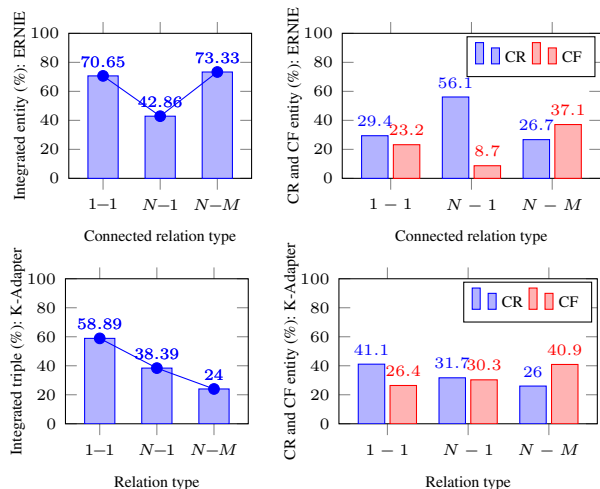


**Figure 7:** Analysis of KI interpretation results in terms of different relation topology.

with complex structure cannot be captured well (Petroni et al., 2019). Regarding CR and CF, we find that for both ERNIE and K-Adapter, CR happens more often to entities in simple structures (i.e.,  $N - 1$  relations), while CF is more common for entities in complex structures (i.e., connected to  $N - M$  relations).

#### 4.3.2. ANALYSIS VIA RELATION’S WIKI FEATURES

**Table 2:** Analysis of KI interpretation results via different relation labels for the T-REx-rc dataset (KI corpus used by K-Adapter).

Relation label	T-REx-rc		
	Wiki Count	Wiki data type	Integrated triple (%)
place of birth (LF)	2,850,424	Wikibase item	10.95%
part of (LF)	4,164,470	Wikibase item	17.25%
date of death (TR)	2,637,358	Time	<0.01%
date of birth (TR)	5,294,649	Time	<0.01%
located in the administrative territorial entity (HF)	10,776,120	Wikibase item	6.13%
country (HF)	14,174,811	Wikibase item	0.12%
Total	-	-	10.09%

We select six relations aligned with roughly the same number of sentences in the T-REx-rc dataset (statistics in Table 9 in Appendix G) and categorize them into three groups based on the *Wiki Count* and *Wiki data type*<sup>9</sup>: low-frequency (LF) relations, time-related (TR) relations, and high-frequency (HF) relations. From Table 2, we find that even if LF relations have roughly the same Wiki Count as TR relations, since the Wiki data type of the latter set is “Time”, triples with those relations cannot be integrated by K-Adapter. We speculate that this is because Transformer encoders do not capture information about time well (Dhingra et al., 2021; Zhou et al., 2021). When comparing LF relations and HF relations, we find that if relations have small Wiki Count, knowledge triples are easier to be captured.

<sup>9</sup>See the [Wikipedia page](#) for more details.

**Table 3:** Examples of knowledge triples in the T-REx-rc dataset (KI corpus used by K-Adapter) and their attention coefficients.

Knowledge triple	Attention coefficient
(Adam Smith, place of birth, Kirkcaldy)	$1.079 \times 10^{-1}$
(Lake Huron, part of, Great Lakes)	$1.742 \times 10^{-1}$
(Jean-Jacques Rousseau, date of death, 02 July 1778)	$1.729 \times 10^{-25}$
(Barack Obama, date of birth, 04 August 1961)	$6.827 \times 10^{-31}$
(Mauna Kea Observatory, located in the administrative territorial entity, Hawaii)	$6.044 \times 10^{-2}$
(China, country, Mahalangur Himal)	$1.250 \times 10^{-3}$

Examples<sup>10</sup> of knowledge triples are given in Table 3. We can find that for TR relations, they connect entities composed of numbers. Considering the poor performance of language models on handling numbers (Wallace et al., 2019), it provides an alternative explanation for the fact that K-Adapter does not integrate triples with TR relations. Regarding triples with LF and HF relations, we can find that some entities connected to HF relations are very common (e.g. entity “China” is in the complex KG structure) compared to those connected to LF relations. The results are consistent with our findings in Figure 7 that common factual knowledge is not integrated well.

Above experiments show that interpretation results of GCS are consistent with existing analysis works, which also verify GCS indirectly. We design another case study experiment in Appendix H.3, where we find that CR often happens to rare entities (small Google Ngrams), while CF often happens to popular entities (large Google Ngrams).

#### 4.3.3. CAN WE IMPROVE THE KI QUALITY?

Previous results analyze KI in LMs in different ways. However, there is a key question: can we simply improve the quality of KI by increasing the amount of our aligned training corpora? We answer this question by calculating the correlation between the attention coefficients and the number of aligned sentences for knowledge triples in the dataset. We find that the *Pearson correlation* between the two is  $-0.0055$  (detailed results in Figure 10 in Appendix G). This implies that there is no apparent positive relationship between the KI quality and the size of the KI dataset. It suggests that simply increasing the size of the aligned dataset alone may not improve KI, but, we might need more fundamental advances to push the state-of-the-art in KI.

## 5. Limitations and Future Work

In this paper, through a series of theoretical results, we illustrate that the graph attention can be used to interpret the KI process for knowledge-enhanced LMs, and thus propose a Graph Convolutional Simulator (GCS) that is capable of correctly interpreting existing knowledge-enhanced LMs. In our experiments, we verify GCS and use it to obtain

<sup>10</sup>We randomly pick triples with attention coefficients close to the integrated triple ratio.

interesting findings<sup>11</sup>.

There are some limitations of our work. We simplify the KG without considering relation information such as labels, since existing graph neural networks (e.g., R-GCN (Schlichtkrull et al., 2018)) still cannot handle such large number of relation types<sup>12</sup>. These can be considered by future works. GCS only provides a way to interpret the knowledge integration. Once we have an understanding of the KI process, improving the integration quality still remains challenging.

## References

- Agarwal, O., Ge, H., Shakeri, S., and Al-Rfou, R. Knowledge graph based synthetic corpus generation for knowledge-enhanced language model pre-training. In Toutanova, K., Rumshisky, A., Zettlemoyer, L., Hakkani-Tür, D., Beltagy, I., Bethard, S., Cotterell, R., Chakraborty, T., and Zhou, Y. (eds.), *NAACL-HLT*, pp. 3554–3565. Association for Computational Linguistics, 2021. doi: 10.18653/v1/2021.naacl-main.278. URL <https://doi.org/10.18653/v1/2021.naacl-main.278>.
- Banerjee, A. On bayesian bounds. In Cohen, W. W. and Moore, A. W. (eds.), *ICML*, volume 148 of *ACM International Conference Proceeding Series*, pp. 81–88. ACM, 2006. doi: 10.1145/1143844.1143855. URL <https://doi.org/10.1145/1143844.1143855>.
- Belghazi, M. I., Baratin, A., Rajeswar, S., Ozair, S., Bengio, Y., Hjelm, R. D., and Courville, A. C. Mutual information neural estimation. In Dy, J. G. and Krause, A. (eds.), *ICML*, volume 80 of *Proceedings of Machine Learning Research*, pp. 530–539. PMLR, 2018. URL <http://proceedings.mlr.press/v80/belghazi18a.html>.
- Bordes, A., Usunier, N., García-Durán, A., Weston, J., and Yakhnenko, O. Translating embeddings for modeling multi-relational data. In Burges, C. J. C., Bottou, L., Ghahramani, Z., and Weinberger, K. Q. (eds.), *Neural Information Processing Systems*, pp. 2787–2795, 2013. URL <https://proceedings.neurips.cc/paper/2013/hash/1cecc7a77928ca8133fa24680a88d2f9-Abstract.html>.
- Bracewell, R. N. and Bracewell, R. N. *The Fourier transform and its applications*, volume 31999. McGraw-Hill New York, 1986.
- Bruna, J., Zaremba, W., Szlam, A., and LeCun, Y. Spectral networks and locally connected networks on graphs. In Bengio, Y. and LeCun, Y. (eds.), *ICLR*, 2014. URL <http://arxiv.org/abs/1312.6203>.
- Chen, Z., Villar, S., Chen, L., and Bruna, J. On the equivalence between graph isomorphism testing and function approximation with gnns. In Wallach, H. M., Larochelle, H., Beygelzimer, A., d’Alché-Buc, F., Fox, E. B., and Garnett, R. (eds.), *Advances in Neural Information Processing Systems 32: Annual Conference on Neural Information Processing Systems 2019, NeurIPS 2019, December 8-14, 2019, Vancouver, BC, Canada*, pp. 15868–15876, 2019. URL <https://proceedings.neurips.cc/paper/2019/hash/71ee911dd06428a96c143a0b135041a4-Abstract.html>.
- Choi, E., Levy, O., Choi, Y., and Zettlemoyer, L. Ultra-fine entity typing. In Gurevych, I. and Miyao, Y. (eds.), *ACL*, pp. 87–96. Association for Computational Linguistics, 2018. doi: 10.18653/v1/P18-1009. URL <https://aclanthology.org/P18-1009/>.
- Colon-Hernandez, P., Havasi, C., Alonso, J. B., Huggins, M., and Breazeal, C. Combining pre-trained language models and structured knowledge. *CoRR*, abs/2101.12294, 2021. URL <https://arxiv.org/abs/2101.12294>.
- Cybenko, G. Approximation by superpositions of a sigmoidal function. *Math. Control. Signals Syst.*, 5(4): 455, 1992. doi: 10.1007/BF02134016. URL <https://doi.org/10.1007/BF02134016>.
- Defferrard, M., Bresson, X., and Vandergheynst, P. Convolutional neural networks on graphs with fast localized spectral filtering. In Lee, D. D., Sugiyama, M., von Luxburg, U., Guyon, I., and Garnett, R. (eds.), *Neural Information Processing Systems*, pp. 3837–3845, 2016. URL <https://proceedings.neurips.cc/paper/2016/hash/04df4d434d481c5bb723belb6df1ee65-Abstract.html>.
- Devlin, J., Chang, M., Lee, K., and Toutanova, K. BERT: pre-training of deep bidirectional transformers for language understanding. In Burstein, J., Doran, C., and Solorio, T. (eds.), *NAACL-HLT*, pp. 4171–4186. Association for Computational Linguistics, 2019. doi: 10.18653/v1/n19-1423. URL <https://doi.org/10.18653/v1/n19-1423>.
- Dhingra, B., Cole, J. R., Eisenschlos, J. M., Gillick, D., Eisenstein, J., and Cohen, W. W. Time-aware language models as temporal knowledge bases. *CoRR*, abs/2106.15110, 2021. URL <https://arxiv.org/abs/2106.15110>.

<sup>11</sup>We will publish the code after the review process.

<sup>12</sup>In Appendix H.4, we discuss the reason and provide statistics of KGs used by ERNIE and K-Adapter as support.

- ElSahar, H., Vougiouklis, P., Remaci, A., Gravier, C., Hare, J. S., Laforest, F., and Simperl, E. T-rex: A large scale alignment of natural language with knowledge base triples. In Calzolari, N., Choukri, K., Cieri, C., Declerck, T., Goggi, S., Hasida, K., Isahara, H., Maegaard, B., Mariani, J., Mazo, H., Moreno, A., Odijk, J., Piperidis, S., and Tokunaga, T. (eds.), *LREC*. European Language Resources Association (ELRA), 2018. URL <http://www.lrec-conf.org/proceedings/lrec2018/summaries/632.html>.
- Ferragina, P. and Scaiella, U. TAGME: on-the-fly annotation of short text fragments (by wikipedia entities). In Huang, J., Koudas, N., Jones, G. J. F., Wu, X., Collins-Thompson, K., and An, A. (eds.), *CIKM*, pp. 1625–1628. ACM, 2010. doi: 10.1145/1871437.1871689. URL <https://doi.org/10.1145/1871437.1871689>.
- Fu, G., Hou, Y., Zhang, J., Ma, K., Kamhoua, B. F., and Cheng, J. Understanding graph neural networks from graph signal denoising perspectives. *CoRR*, abs/2006.04386, 2020. URL <https://arxiv.org/abs/2006.04386>.
- Guan, C., Wang, X., Zhang, Q., Chen, R., He, D., and Xie, X. Towards a deep and unified understanding of deep neural models in NLP. In Chaudhuri, K. and Salakhutdinov, R. (eds.), *Proceedings of the 36th International Conference on Machine Learning, ICML 2019, 9-15 June 2019, Long Beach, California, USA*, volume 97 of *Proceedings of Machine Learning Research*, pp. 2454–2463. PMLR, 2019. URL <http://proceedings.mlr.press/v97/guan19a.html>.
- Hewitt, J. and Manning, C. D. A structural probe for finding syntax in word representations. In Burstein, J., Doran, C., and Solorio, T. (eds.), *NAACL-HLT*, pp. 4129–4138. Association for Computational Linguistics, 2019. doi: 10.18653/v1/n19-1419. URL <https://doi.org/10.18653/v1/n19-1419>.
- Hou, Y. and Sachan, M. Bird’s eye: Probing for linguistic graph structures with a simple information-theoretic approach. In Zong, C., Xia, F., Li, W., and Navigli, R. (eds.), *ACL/IJCNLP*, pp. 1844–1859. Association for Computational Linguistics, 2021. doi: 10.18653/v1/2021.acl-long.145. URL <https://doi.org/10.18653/v1/2021.acl-long.145>.
- Jawahar, G., Sagot, B., and Seddah, D. What does BERT learn about the structure of language? In Korhonen, A., Traum, D. R., and Màrquez, L. (eds.), *ACL*, pp. 3651–3657. Association for Computational Linguistics, 2019. doi: 10.18653/v1/p19-1356. URL <https://doi.org/10.18653/v1/p19-1356>.
- Kaushik, P., Gain, A., Kortylewski, A., and Yuille, A. L. Understanding catastrophic forgetting and remembering in continual learning with optimal relevance mapping. *CoRR*, abs/2102.11343, 2021. URL <https://arxiv.org/abs/2102.11343>.
- Keriven, N. and Peyré, G. Universal invariant and equivariant graph neural networks. In Wallach, H. M., Larochelle, H., Beygelzimer, A., d’Alché-Buc, F., Fox, E. B., and Garnett, R. (eds.), *Advances in Neural Information Processing Systems 32: Annual Conference on Neural Information Processing Systems 2019, NeurIPS 2019, December 8-14, 2019, Vancouver, BC, Canada*, pp. 7090–7099, 2019. URL <https://proceedings.neurips.cc/paper/2019/hash/ea9268cb43f55d1d12380fb6ea5bf572-Abstract.html>.
- Kipf, T. N. and Welling, M. Semi-supervised classification with graph convolutional networks. In *ICLR*. OpenReview.net, 2017. URL <https://openreview.net/forum?id=SJU4ayYgl>.
- Kirkpatrick, J., Pascanu, R., Rabinowitz, N. C., Veness, J., Desjardins, G., Rusu, A. A., Milan, K., Quan, J., Ramalho, T., Grabska-Barwinska, A., Hassabis, D., Clopath, C., Kumaran, D., and Hadsell, R. Overcoming catastrophic forgetting in neural networks. *CoRR*, abs/1612.00796, 2016. URL <http://arxiv.org/abs/1612.00796>.
- Kraskov, A., Stögbauer, H., and Grassberger, P. Estimating mutual information. *Physical review E*, 69(6):066138, 2004.
- Ling, X., Singh, S., and Weld, D. S. Design challenges for entity linking. *Trans. Assoc. Comput. Linguistics*, 3:315–328, 2015. URL <https://tacl2013.cs.columbia.edu/ojs/index.php/tacl/article/view/528>.
- Liu, N. F., Gardner, M., Belinkov, Y., Peters, M. E., and Smith, N. A. Linguistic knowledge and transferability of contextual representations. In Burstein, J., Doran, C., and Solorio, T. (eds.), *NAACL-HLT*, pp. 1073–1094. Association for Computational Linguistics, 2019a. doi: 10.18653/v1/n19-1112. URL <https://doi.org/10.18653/v1/n19-1112>.
- Liu, W., Zhou, P., Zhao, Z., Wang, Z., Ju, Q., Deng, H., and Wang, P. K-BERT: enabling language representation with knowledge graph. In *AAAI*, pp. 2901–2908. AAAI Press, 2020. URL <https://aaai.org/ojs/index.php/AAAI/article/view/5681>.
- Liu, Y., Ott, M., Goyal, N., Du, J., Joshi, M., Chen, D., Levy, O., Lewis, M., Zettlemoyer, L., and Stoyanov, V. Roberta:

- A robustly optimized BERT pretraining approach. *CoRR*, abs/1907.11692, 2019b. URL <http://arxiv.org/abs/1907.11692>.
- Lu, Y., Lu, H., Fu, G., and Liu, Q. KELM: knowledge enhanced pre-trained language representations with message passing on hierarchical relational graphs. *CoRR*, abs/2109.04223, 2021. URL <https://arxiv.org/abs/2109.04223>.
- Ohn, I. and Kim, Y. Smooth function approximation by deep neural networks with general activation functions. *Entropy*, 21(7):627, 2019. doi: 10.3390/e21070627. URL <https://doi.org/10.3390/e21070627>.
- Parisi, G. I., Kemker, R., Part, J. L., Kanan, C., and Wermter, S. Continual lifelong learning with neural networks: A review. *Neural Networks*, 113:54–71, 2019. doi: 10.1016/j.neunet.2019.01.012. URL <https://doi.org/10.1016/j.neunet.2019.01.012>.
- Perozzi, B., Al-Rfou, R., and Skiena, S. Deepwalk: online learning of social representations. In Macskassy, S. A., Perlich, C., Leskovec, J., Wang, W., and Ghani, R. (eds.), *The 20th ACM SIGKDD International Conference on Knowledge Discovery and Data Mining, KDD '14, New York, NY, USA - August 24 - 27, 2014*, pp. 701–710. ACM, 2014. doi: 10.1145/2623330.2623732. URL <https://doi.org/10.1145/2623330.2623732>.
- Peters, M. E., Neumann, M., IV, R. L. L., Schwartz, R., Joshi, V., Singh, S., and Smith, N. A. Knowledge enhanced contextual word representations. In Inui, K., Jiang, J., Ng, V., and Wan, X. (eds.), *EMNLP-IJCNLP*, pp. 43–54. Association for Computational Linguistics, 2019. doi: 10.18653/v1/D19-1005. URL <https://doi.org/10.18653/v1/D19-1005>.
- Petroni, F., Rocktäschel, T., Riedel, S., Lewis, P. S. H., Bakhtin, A., Wu, Y., and Miller, A. H. Language models as knowledge bases? In Inui, K., Jiang, J., Ng, V., and Wan, X. (eds.), *EMNLP-IJCNLP*, pp. 2463–2473. Association for Computational Linguistics, 2019. doi: 10.18653/v1/D19-1250. URL <https://doi.org/10.18653/v1/D19-1250>.
- Pimentel, T., Valvoda, J., Maudslay, R. H., Zmigrod, R., Williams, A., and Cotterell, R. Information-theoretic probing for linguistic structure. In Jurafsky, D., Chai, J., Schluter, N., and Tetreault, J. R. (eds.), *ACL*. Association for Computational Linguistics, 2020. doi: 10.18653/v1/2020.acl-main.420. URL <https://doi.org/10.18653/v1/2020.acl-main.420>.
- Ribeiro, M. T., Singh, S., and Guestrin, C. "why should I trust you?": Explaining the predictions of any classifier. In Krishnapuram, B., Shah, M., Smola, A. J., Aggarwal, C. C., Shen, D., and Rastogi, R. (eds.), *Proceedings of the 22nd ACM SIGKDD International Conference on Knowledge Discovery and Data Mining, San Francisco, CA, USA, August 13-17, 2016*, pp. 1135–1144. ACM, 2016. doi: 10.1145/2939672.2939778. URL <https://doi.org/10.1145/2939672.2939778>.
- Sandryhaila, A. and Moura, J. M. F. Discrete signal processing on graphs: Frequency analysis. *IEEE Trans. Signal Process.*, 62(12):3042–3054, 2014. doi: 10.1109/TSP.2014.2321121. URL <https://doi.org/10.1109/TSP.2014.2321121>.
- Schlichtkrull, M. S., Kipf, T. N., Bloem, P., van den Berg, R., Titov, I., and Welling, M. Modeling relational data with graph convolutional networks. In Gangemi, A., Navigli, R., Vidal, M., Hitzler, P., Troncy, R., Hollink, L., Tordai, A., and Alam, M. (eds.), *The Semantic Web - 15th International Conference, ESWC 2018, Heraklion, Crete, Greece, June 3-7, 2018, Proceedings*, volume 10843 of *Lecture Notes in Computer Science*, pp. 593–607. Springer, 2018. doi: 10.1007/978-3-319-93417-4\_38. URL [https://doi.org/10.1007/978-3-319-93417-4\\_38](https://doi.org/10.1007/978-3-319-93417-4_38).
- Schlichtkrull, M. S., Cao, N. D., and Titov, I. Interpreting graph neural networks for NLP with differentiable edge masking. *CoRR*, abs/2010.00577, 2020. URL <https://arxiv.org/abs/2010.00577>.
- Shin, T., Razeghi, Y., IV, R. L. L., Wallace, E., and Singh, S. Autoprompt: Eliciting knowledge from language models with automatically generated prompts. In Weber, B., Cohn, T., He, Y., and Liu, Y. (eds.), *Proceedings of the 2020 Conference on Empirical Methods in Natural Language Processing, EMNLP 2020, Online, November 16-20, 2020*, pp. 4222–4235. Association for Computational Linguistics, 2020. doi: 10.18653/v1/2020.emnlp-main.346. URL <https://doi.org/10.18653/v1/2020.emnlp-main.346>.
- Tang, Y., Huang, J., Wang, G., He, X., and Zhou, B. Orthogonal relation transforms with graph context modeling for knowledge graph embedding. In Jurafsky, D., Chai, J., Schluter, N., and Tetreault, J. R. (eds.), *Proceedings of the 58th Annual Meeting of the Association for Computational Linguistics, ACL 2020, Online, July 5-10, 2020*, pp. 2713–2722. Association for Computational Linguistics, 2020. doi: 10.18653/v1/2020.acl-main.241. URL <https://doi.org/10.18653/v1/2020.acl-main.241>.
- Thekumparampil, K. K., Wang, C., Oh, S., and Li, L. Attention-based graph neural network for semi-supervised learning. *CoRR*, abs/1803.03735, 2018. URL <http://arxiv.org/abs/1803.03735>.

- Vaswani, A., Shazeer, N., Parmar, N., Uszkoreit, J., Jones, L., Gomez, A. N., Kaiser, L., and Polosukhin, I. Attention is all you need. In Guyon, I., von Luxburg, U., Bengio, S., Wallach, H. M., Fergus, R., Vishwanathan, S. V. N., and Garnett, R. (eds.), *Neural Information Processing Systems*, pp. 5998–6008, 2017. URL <https://proceedings.neurips.cc/paper/2017/hash/3f5ee243547dee91fbd053c1c4a845aa-Abstract.html>.
- Velickovic, P., Cucurull, G., Casanova, A., Romero, A., Liò, P., and Bengio, Y. Graph attention networks. In *ICLR OpenReview.net*, 2018. URL <https://openreview.net/forum?id=rJXMpikCZ>.
- Wallace, E., Wang, Y., Li, S., Singh, S., and Gardner, M. Do NLP models know numbers? probing numeracy in embeddings. In Inui, K., Jiang, J., Ng, V., and Wan, X. (eds.), *Proceedings of the 2019 Conference on Empirical Methods in Natural Language Processing and the 9th International Joint Conference on Natural Language Processing, EMNLP-IJCNLP 2019, Hong Kong, China, November 3-7, 2019*, pp. 5306–5314. Association for Computational Linguistics, 2019. doi: 10.18653/v1/D19-1534. URL <https://doi.org/10.18653/v1/D19-1534>.
- Wang, R., Tang, D., Duan, N., Wei, Z., Huang, X., Ji, J., Cao, G., Jiang, D., and Zhou, M. K-adapter: Infusing knowledge into pre-trained models with adapters. In Zong, C., Xia, F., Li, W., and Navigli, R. (eds.), *Findings of ACL/IJCNLP*, volume ACL/IJCNLP 2021 of *Findings of ACL*, pp. 1405–1418. Association for Computational Linguistics, 2021a. doi: 10.18653/v1/2021.findings-acl.121. URL <https://doi.org/10.18653/v1/2021.findings-acl.121>.
- Wang, X., Gao, T., Zhu, Z., Zhang, Z., Liu, Z., Li, J., and Tang, J. KEPLER: A unified model for knowledge embedding and pre-trained language representation. *Trans. Assoc. Comput. Linguistics*, 9:176–194, 2021b. URL <https://transacl.org/ojs/index.php/tacl/article/view/2447>.
- Yao, L., Mao, C., and Luo, Y. KG-BERT: BERT for knowledge graph completion. *CoRR*, abs/1909.03193, 2019. URL <http://arxiv.org/abs/1909.03193>.
- Zhang, Z., Han, X., Liu, Z., Jiang, X., Sun, M., and Liu, Q. ERNIE: enhanced language representation with informative entities. In Korhonen, A., Traum, D. R., and Màrquez, L. (eds.), *ACL*, pp. 1441–1451. Association for Computational Linguistics, 2019. doi: 10.18653/v1/p19-1139. URL <https://doi.org/10.18653/v1/p19-1139>.
- Zhong, Z., Friedman, D., and Chen, D. Factual probing is [MASK]: learning vs. learning to recall. In Toutanova, K., Rumshisky, A., Zettlemoyer, L., Hakkani-Tür, D., Beltagy, I., Bethard, S., Cotterell, R., Chakraborty, T., and Zhou, Y. (eds.), *Proceedings of the 2021 Conference of the North American Chapter of the Association for Computational Linguistics: Human Language Technologies, NAACL-HLT 2021, Online, June 6-11, 2021*, pp. 5017–5033. Association for Computational Linguistics, 2021. doi: 10.18653/v1/2021.naacl-main.398. URL <https://doi.org/10.18653/v1/2021.naacl-main.398>.
- Zhou, B., Richardson, K., Ning, Q., Khot, T., Sabharwal, A., and Roth, D. Temporal reasoning on implicit events from distant supervision. In Toutanova, K., Rumshisky, A., Zettlemoyer, L., Hakkani-Tür, D., Beltagy, I., Bethard, S., Cotterell, R., Chakraborty, T., and Zhou, Y. (eds.), *NAACL-HLT*, pp. 1361–1371. Association for Computational Linguistics, 2021. doi: 10.18653/v1/2021.naacl-main.107. URL <https://doi.org/10.18653/v1/2021.naacl-main.107>.

## A. Notations

Table 4: Notations and their descriptions

Notation	Description
$\mathcal{G}$	The knowledge graph for KI
$\mathcal{V}$	The set of entities/nodes of KG
$\mathcal{E}$	The set of relations/edges of KG
$v_i$	The entity/node indexed as $i$ in the KG
$t_i$	The entity text attached on $v_i$
$\text{LM}(\cdot)$	The language model, where the input is entity text, and the output is its representation
$\mathcal{N}_{v_i}$	The set of neighbors (entities/nodes) connected to $v_i$
$\mathcal{G}(v_i)$	The local graph structure in terms of $v_i$
$\mathbf{x}$	The random variable of the entity representation
$\mathbf{x}_i$	The entity representations of $v_i$
$\mathbf{g}$	The random variable of the local graph structure
$\text{MI}(\cdot; \cdot)$	The mutual information between two random variables
$\mathbf{A}$	The adjacency matrix of KG
$ \mathcal{V} $	The number of entities/nodes in KG
$\mathbb{R}$	The set of real numbers
$\mathbf{I}$	The identity matrix
$\mathbf{D}$	The degree matrix of KG
$\mathbf{L}_n$	The normalized Laplacian matrix
$\text{diag}(\cdot)$	The diagonalization operation
$\mathbf{U}$	The matrix of eigenvectors
$\mathbf{\Lambda}$	The diagonal matrix of eigenvalues
$\lambda_i$	The $i$ -th eigenvalue
$\mathbf{X}$	The set of entity representations in terms of $\mathcal{V}$
$C$	The dimension of entity representations; The number of channels
$\text{GFT}(\cdot)$	The graph Fourier transformation
$\text{RGFT}(\cdot)$	The inverse graph Fourier transformation
$g_\Theta$	The graph filter parameterized by parameter $\Theta$
$\mathbf{H}$	The entity representations given by a knowledge-enhanced LM
$\mathbf{h}$	The random variable of the entity representation given by a knowledge-enhanced LM
$f(\cdot)$	The mapping that can transform $\mathbf{x}$ to $\mathbf{h}$
$\epsilon$	The error of the approximation
$\text{sigmoid}(\mathbf{x})$	The Sigmoid function $\text{sigmoid}(\cdot) = \frac{1}{1+e^{-x}}$
$n$	The number of layers of the neural network for approximation
$\mathbf{W}$	The weight matrix
$\mathbf{x}$	The input vector
$\mathbf{b}$	The bias
$\lambda'_0$	The minimum eigenvalue of the weight matrix $\mathbf{W}$
$\text{MLP}_n(\cdot)$	The bijective MLP function
$\text{GC}(\cdot, \cdot)$	The graph convolution function
$\text{GCS}_{\theta_1}$	The GCS model parameterized by $\theta_1$
$\mathcal{L}$	The objective of the optimization
$\mathbf{Z}$	The output of GCS, i.e., set of output entity representations
$\mathbf{z}$	The random variable of the output of GCS
$\sup$	The supremum value
$T$	A class of functions
$\mathcal{F}$	Any class of functions
$\Omega$	The domain of a function
$T_{\theta_2}$	A class of functions parameterized by $\theta_2$ , i.e., neural networks
$\mathbb{P}$	The probability distribution
$\mathbb{P}^{ \mathcal{V} }$	The empirical distribution with $ \mathcal{V} $ samples
$\text{NN}_\sigma(\cdot \theta')$	The neural network with activation function $\sigma(\cdot)$ and parameterized by $\theta'$
$ \mathbf{U} $	The norm of matrix $\mathbf{U}$
$\mathbf{A}_n$	The normalized adjacency matrix
$\hat{\mathbf{X}}$	The ground-truth entity representations/node features
$\hat{\mathbf{X}}^*$	The variable matrix
$\text{Tr}(\cdot)$	The trace of a matrix
$\epsilon_1, \epsilon_2$	The error bound of entity representations/node features and adjacency matrix
$\gamma$	The Lagrangian multiplier
$p(t)$	The characteristic polynomial for weight matrix $\mathbf{W}$
$\det(\cdot)$	The determinant of a matrix

## B. Proof of Theorem 2.2

*Proof.* As aforementioned, the graph Fourier transformation  $\text{GFT}(\cdot)$  and its inverse transformation  $\text{RGFT}(\cdot)$  in terms of the KG  $\mathcal{G}$  can be written as

$$\begin{aligned}\text{GFT}(\mathbf{X}) &= \mathbf{U}^T \mathbf{X} \\ \text{RGFT}(\text{GFT}(\mathbf{X})) &= \mathbf{U} \text{GFT}(\mathbf{X}) = \mathbf{U} \mathbf{U}^T \mathbf{X} = \mathbf{X}.\end{aligned}$$

The second equation can be derived since  $\mathbf{U}$  is the set of eigenvectors of the normalized Laplacian matrix in terms of  $\mathcal{G}$ , which is orthogonal.

According to the universal approximation theorem (Cybenko, 1992), in general, we can use one-layer neural networks (arbitrary width) with the sigmoid activation function to fit any functions. Ohn & Kim (2019) bound the approximation with both the width and depth, and supports more activation functions. Based on the conclusion of Ohn & Kim (2019), we know that given a mapping  $f'(\cdot)$ , for any  $\epsilon' > 0$ , there exists a neural network parameterized by  $\theta'$  s.t.

$$|f'(\cdot) - \text{NN}_\sigma(\cdot|\theta')| < \epsilon'.$$

Note that there are some constraints about the input and the model architecture, i.e., width and depth. We leave out those details for simplicity. More details can be found in Ohn & Kim (2019).

Since  $\mathbf{h}$  is obtained by integrating  $\mathbf{g}$  into  $\mathbf{x}$ , we can simplify the mapping in the graph space by researching on the transformation from  $\text{GFT}(\mathbf{x})$  to  $\text{GFT}(\mathbf{h})$ <sup>13</sup>. Assume the mapping satisfies  $f'(\text{GFT}(\mathbf{x})) = \text{GFT}(\mathbf{h})$ . Then we have

$$|f'(\text{GFT}(\mathbf{x})) - \text{NN}_\sigma(\text{GFT}(\mathbf{x})|\theta')| < \epsilon'.$$

Consider that we have  $f(\mathbf{x}, \mathbf{g}) = \mathbf{h} = \text{RGFT}(f'(\text{GFT}(\mathbf{x})))$ . If we assign  $\epsilon' = \frac{\epsilon}{|\mathbf{U}|} > 0$ , we have

$$|\mathbf{U}| \cdot |f'(\text{GFT}(\mathbf{x})) - \text{NN}_\sigma(\text{GFT}(\mathbf{x})|\theta')| < \epsilon.$$

Since we know that

$$\mathbf{U} \cdot f'(\text{GFT}(\mathbf{x})) = \text{RGFT}(f'(\text{GFT}(\mathbf{x}))) = \mathbf{h} = f(\mathbf{x}, \mathbf{g}),$$

we have

$$|f(\mathbf{x}, \mathbf{g}) - \text{RGFT}(\text{NN}(\text{GFT}(\mathbf{x})))| < |\mathbf{U}| \cdot |f'(\text{GFT}(\mathbf{x})) - \text{NN}_\sigma(\text{GFT}(\mathbf{x})|\theta')| < \epsilon,$$

where  $\text{NN}(\cdot)$  is parameterized by  $\theta'$  with activation function  $\sigma$  as  $\text{NN}_\sigma(\cdot|\theta')$ . And without loss of generality, we assume it is composed of  $n$  layers.  $\square$

## C. Proof of Proposition 2.3

*Proof.* The basic idea of this proof can be found in Figure 2. We first simply prove that the graph Fourier transformation is bijective. Similarly, the nonlinear activation function can be proved bijective. Then, we show that information gain and loss can only happen in the linear function in graph space. After that, we briefly illustrate that linear function in graph space is graph convolution operation. Finally, we prove that graph attention works as edge denoising, and we can use it to interpret the KI.

### C.1. Step 1

$\text{GFT}(\cdot)$ ,  $\text{RGFT}(\cdot)$ , and  $\text{sigmoid}(\cdot)$  are bijective. Given two entity representations  $\mathbf{x}_i$ ,  $\mathbf{x}_j$  and the matrix of eigenvectors of the KG as  $\mathbf{U}$ , suppose that  $\text{GFT}(\mathbf{x}_i) = \text{GFT}(\mathbf{x}_j)$ . Then, we have

$$\mathbf{U}^T \mathbf{x}_i = \mathbf{U}^T \mathbf{x}_j.$$

<sup>13</sup>In next proof, we illustrate that the linear transformation in the graph space is graph convolution, which integrates the graph information into entities. Thus, in the graph space, we do not need to regard  $\mathbf{g}$  as an input. More formally description can be found in Chen et al. (2019); Keriven & Peyré (2019).

Since  $U^T$  are set of eigenvectors and are by definition nonzero, we have

$$\mathbf{x}_i = \mathbf{x}_j.$$

If  $\mathbf{x}_i = \mathbf{x}_j$ , it is easy to get  $\text{GFT}(\mathbf{x}_i) = \text{GFT}(\mathbf{x}_j)$ . Thus, graph Fourier transformation is bijective.

As for the nonlinear activation function, since we consider neural networks composed of MLP layers, the activation function is sigmoid( $\cdot$ ) function. It is easy to find that its inverse function is  $f(\mathbf{y}) = \ln(1 - \frac{1}{\mathbf{y}})$ . Similarly, we can prove that it is bijective as well.

## C.2. Step 2

**Information gain and loss can only happen in the linear function in graph space.** Based on the invariance of MI (Kaskov et al., 2004), we have

$$\begin{aligned} \text{MI}(\mathbf{x}, \mathbf{g}) &= \text{MI}(\text{GFT}(\mathbf{x}), \mathbf{g}), \\ \text{MI}(\mathbf{x}, \mathbf{g}) &= \text{MI}(\text{RGFT}(\mathbf{x}), \mathbf{g}), \\ \text{MI}(\mathbf{x}, \mathbf{g}) &= \text{MI}(\text{sigmoid}(\mathbf{x}), \mathbf{g}). \end{aligned} \quad (5)$$

Since we know that

$$\text{MI}(\mathbf{h}, \mathbf{g}) - \text{MI}(\mathbf{x}, \mathbf{g}) > 0,$$

and the neural network can well approximate the mapping, we have

$$\begin{aligned} \text{MI}(\mathbf{h}, \mathbf{g}) - \text{MI}(\mathbf{x}, \mathbf{g}) &\approx \text{MI}(\text{RGFT}(\text{NN}(\text{GFT}(\mathbf{x}))), \mathbf{g}) - \text{MI}(\mathbf{x}, \mathbf{g}) \\ &= \text{MI}(\text{NN}(\text{GFT}(\mathbf{x})), \mathbf{g}) - \text{MI}(\text{GFT}(\mathbf{x}), \mathbf{g}) > 0. \end{aligned}$$

If we write  $\text{NN}(\cdot)$  with  $n$  MLP layers as  $n \times \sigma(\text{Linear}(\cdot))$ , we have

$$\text{MI}(n \times \sigma(\text{Linear}(\text{GFT}(\mathbf{x}))), \mathbf{g}) - \text{MI}(\text{GFT}(\mathbf{x}), \mathbf{g}) > 0.$$

Recursively with equations 5, it is easy to get that MI only changes in the  $\text{Linear}(\cdot)$  functions.

## C.3. Step 3

**The linear function in the KG space (i.e., graph spectral domain) is the graph convolution operation.** Even if many existing works (Sandryhaila & Moura, 2014; Bruna et al., 2014; Kipf & Welling, 2017) have provided clear descriptions, we simply re-illustrate it under the multi-channel setting. Consider the graph filter in Bruna et al. (2014) as an example.

For a linear function  $f(\mathbf{x}) = \mathbf{W} \times \mathbf{x}$ , its weight matrix  $\mathbf{W} \in \mathbb{R}^{F \times C}$  is parameterized by  $\Theta \in \mathbb{R}^{F \times C}$ . If the parameters are not shared for all nodes, the input  $\mathbf{X} \in \mathbb{R}^{|\mathcal{V}| \times C}$  can be rescaled in  $\mathbb{R}^{|\mathcal{V}| \times C \times 1}$ , and the weight matrix is  $\mathbf{W} \in \mathbb{R}^{|\mathcal{V}| \times F \times C}$  parameterized by  $\Theta \in \mathbb{R}^{F \times C \times |\mathcal{V}|}$ . The output of this linear function is mapped in  $\mathbb{R}^{|\mathcal{V}| \times F}$ .

Consider the signal in graph convolution, i.e., all  $\mathbf{x}$  in  $\mathbf{X} \in \mathbb{R}^{|\mathcal{V}| \times C}$ . Since parameters are not shared (Bruna et al., 2014), for one graph filter, the parameters in  $g_\Theta$  is in  $\mathbb{R}^{C \times |\mathcal{V}| \times |\mathcal{V}|}$  that is parameterized by  $\Theta \in \mathbb{R}^{C \times |\mathcal{V}|}$  with simple diagonalization. If we have  $F$  different graph filters for the convolution,  $g_\Theta$  is in  $\mathbb{R}^{F \times C \times |\mathcal{V}| \times |\mathcal{V}|}$  that is parameterized by  $\Theta \in \mathbb{R}^{F \times C \times |\mathcal{V}|}$ . Here, the graph Fourier transformation of  $\mathbf{X}$  is  $\text{GFT}(\mathbf{X}) \in \mathbb{R}^{|\mathcal{V}| \times C}$ , which can be rescaled in  $\mathbb{R}^{1 \times |\mathcal{V}| \times C \times 1}$  with simple diagonalization. The output is in  $\mathbb{R}^{F \times |\mathcal{V}| \times |\mathcal{V}| \times 1}$ . Note that since the parameters in the graph filter is diagonalized, we can rescale the output in  $\mathbb{R}^{|\mathcal{V}| \times F}$ .

If we regard the weight matrix  $\mathbf{W}$  as the parameters in the graph filter  $g_\Theta$ , the input matrix  $\mathbf{X}$  as the signal, obviously, the linear function in the graph space is the graph convolution operation.  $\square$

## D. Proof of Proposition 3.1

*Proof.* **Graph attention works as edge denoising**<sup>14</sup>. Graph attention works as a better graph convolution filter, since it can adaptively learn the optimal convolution weights (i.e., attention coefficients). Consider a graph signal denoising problem

<sup>14</sup>The detailed proof can be found in Fu et al. (2020).

that we aim to extract the ground-truth node features  $\hat{\mathbf{X}}$  and edge weights  $\hat{\mathbf{A}}_n$  from a graph  $\mathcal{G} = (\mathcal{V}, \mathcal{E}, \mathbf{A}_n)$  with noise in both node features  $\mathbf{X}$  and edge weights  $\mathbf{A}_n$ . Here,  $\mathbf{A}_n$  is the normalized adjacency matrix  $\mathbf{A}_n = \mathbf{D}^{-1/2} \mathbf{A} \mathbf{D}^{-1/2}$ . To this end, we formulate the optimization problem under the assumption that the ground-truth node features  $\hat{\mathbf{X}}$  are smooth w.r.t the ground-truth adjacency matrix  $\hat{\mathbf{A}}_n$  and the noise in the graph can be upper-bounded:

$$\begin{aligned} \hat{\mathbf{X}}^*, \hat{\mathbf{A}}_n^* &= \underset{\hat{\mathbf{X}}, \hat{\mathbf{A}}_n}{\operatorname{argmin}} \operatorname{Tr} \left( \hat{\mathbf{X}} \hat{\mathbf{L}}_n^T \hat{\mathbf{X}} \right) \\ \text{s.t. } &\|\hat{\mathbf{X}} - \mathbf{X}\|_2^2 \leq \epsilon_1, \\ &\|\hat{\mathbf{A}}_n - \mathbf{A}_n\|_2^2 \leq \epsilon_2, \end{aligned} \quad (6)$$

where  $\hat{\mathbf{L}} = \mathbf{I} - \hat{\mathbf{A}}$ ,  $\epsilon_1, \epsilon_2 \in \mathbb{R}$ , are the level of noise in node features and edge weights, respectively.  $\operatorname{Tr}(\cdot)$  indicates the trace of a matrix. By Lagrange multipliers methods, we can obtain the solution as following:

$$\hat{\mathbf{X}}^* = \frac{\gamma}{1 + \gamma} \left( \mathbf{I} - \frac{1}{1 + \gamma} \hat{\mathbf{A}}_n^* \right), \quad (7)$$

$$\hat{\mathbf{A}}_n^* = \mathbf{A}_n + \sqrt{\epsilon_2} \frac{\hat{\mathbf{X}}^* \hat{\mathbf{X}}^{*\top}}{\|\hat{\mathbf{X}}^*\|_2^2}, \quad (8)$$

where  $\gamma > 0$  is the Lagrangian multiplier. Note that the attention coefficients of GAT (Velickovic et al., 2018) and AGNN (Thekumparampil et al., 2018) are obtained by (without less of generality, we show the results in the first-layer) equation 9 and equation 10, respectively:

$$a_{i,j} = \operatorname{softmax} \left( \operatorname{leakyReLU} \left( \mathbf{a}^\top [\mathbf{W} \mathbf{X}_i \| \mathbf{W} \mathbf{X}_j] \right)_{j \in \mathcal{N}_i \cup \{i\}} \right), \quad (9)$$

$$a_{i,j} = \operatorname{softmax} \left( \left[ \beta \frac{\mathbf{H}_i^\top \mathbf{H}_j}{\|\mathbf{H}_i\| \|\mathbf{H}_j\|} \right]_{j \in \mathcal{N}_i \cup \{i\}} \right), \quad (10)$$

where  $\mathbf{H} = \operatorname{ReLU}(\mathbf{X} \mathbf{W})$ ,  $\mathbf{a}, \mathbf{W}$  in equation 9, and  $\beta, \mathbf{W}$  in equation 10 are learnable parameters. The attention coefficients of GAT and AGNN are then used as the weights of aggregating the neighborhood information of nodes. As we can see that equation 8, equation 9, and equation 10 are in a form of measuring the similarity between paired node features. Similar to the denoised edge weights obtained in equation 8, the attention coefficients (i.e. the aggregation weights) between a node and its neighborhoods are proportional to the similarity of their node embeddings. Therefore, the attention coefficients of GAT and AGNN can be regarded as the results of denoised weights on the existing edges in a graph, i.e., the graph attentions are implicitly denoising the edge weights.

In general case, graph attention functions as denoising edge weights. The input is noisy representations and the output is the groundtruth. Attention coefficients show how much distortion is corrected during the convolution operation. For example, if the input representations are also groundtruth, there is no need to fetch information from neighbors to get output. And edge weights will be reduced to 0, i.e., attention coefficients on edges are calculated as 0. If the input representations are very noisy, i.e., much noise are removed, attention coefficients on edges should be large to restore the groundtruth signal. Therefore, in the KI scenario, we can use attention coefficients in graph attention in graph convolution layer to interpret the KI process such as how much triple information is integrated. As for the CR and CF, equally, we can use the attention coefficients on the self-loop edges for interpretation, such as how much original information is remembered/forgotten.  $\square$

## E. Proof: MLP Can be Bijective

**Theorem E.1.** *Give an MLP layer denoted as  $\operatorname{MLP}(\mathbf{x}) = \operatorname{sigmoid}(\mathbf{W} \mathbf{x} + \mathbf{b})$ . If  $\mathbf{W}$  is a square matrix, there exist a constant  $\lambda'_0 > 0$  that for any  $0 < \epsilon < \lambda'_0$ , the function below is bijective:*

$$\operatorname{MLP}_n(\mathbf{x}) = \operatorname{sigmoid}((\mathbf{W} - \epsilon \mathbf{I}) \mathbf{x} + \mathbf{b}). \quad (11)$$

*Proof.* We first prove that two bijective function compositions are still bijective. Then, we prove that adding a small noise on MLP weight matrix can make it bijective.

Give two function  $f_1(\cdot)$  and  $f_2(\cdot)$ . Suppose they are injective and suppose  $f_1(f_2(\mathbf{x})) = f_1(f_2(\mathbf{y}))$ . Since we know that  $f_1(\cdot)$  is injective, we have  $f_2(\mathbf{x}) = f_2(\mathbf{y})$ . Similarly, since  $f_2(\cdot)$  is injective, we have  $\mathbf{x} = \mathbf{y}$ . Thus  $f_1(f_2(\cdot))$  is injective. Suppose  $f_1(\cdot)$  and  $f_2(\cdot)$  are surjective and  $\mathbf{z} \in C$ . Since we know that  $f_1(\cdot)$  is surjective, there exists a set of  $\mathbf{y} \in B$  with  $f_1(\mathbf{y}) = \mathbf{z}$ . Similarly, since  $f_2(\cdot)$  is surjective, there exists a set of  $\mathbf{x} \in A$  with  $f_2(\mathbf{x}) = \mathbf{y}$ . Then, we have  $\mathbf{z} = f_1(f_2(\mathbf{x}))$  and so  $\mathbf{z}$  is onto  $f_1(f_2(\cdot))$ . Thus,  $f_1(f_2(\cdot))$  is surjective. Therefore, if  $f_1(\cdot)$  and  $f_2(\cdot)$  are bijective,  $f_1(f_2(\cdot))$  is also bijective.

To prove that the special MLP is bijective, consider an MLP function as

$$\text{MLP}(\mathbf{x}) = \sigma(\mathbf{W}\mathbf{x} + \mathbf{b}),$$

where  $\mathbf{W} \in \mathbb{R}^{C \times C}$  is the weight matrix and  $\mathbf{b} \in \mathbb{R}^C$  is the bias. Let

$$p(t) = \prod_{i=1}^C (\lambda'_i - t)$$

be the characteristic polynomial for weight matrix  $\mathbf{W}$ . Here  $\lambda'_i$  are eigenvalues of matrix  $\mathbf{W}$ . Without loss of generality, let  $|\lambda'_0| = \min_i |\lambda'_i|$ . Then, we know that for any constant  $0 < \epsilon < |\lambda'_0|$ , we have

$$\det(\mathbf{W} - \epsilon \mathbf{I}) = p(\epsilon) \neq 0.$$

Thus, if the perturbation  $\epsilon$  is small enough, the perturbed matrix  $\mathbf{W}' = \mathbf{W} - \epsilon \mathbf{I}$  is nonsingular. Consider the fact that the nonlinear activation function  $\sigma(\cdot)$  is sigmoid( $\cdot$ ) function, which is bijective. Therefore, the special MLP function  $\text{MLP}_n(\cdot)$  is bijective. And there is no information loss.  $\square$

## F. Implementation Details

### F.1. Synthetic Experiment

**DeepWalk.** We implement DeepWalk to get KG embeddings. The hyperparameters are set as the same as its default values<sup>15</sup>: the number of walks is set as 10, and the walk length is set as 40. The dimension of embeddings is set as 128. Note that since knowledge triples only contain neighbors within one-hop, we select the window size as 1.

**Noisy KG embeddings.** We add Gaussian noisy on the KG embeddings with different ratios. For example, if we add 10% ratio of noise, it can be written as

$$10\% \text{ noisy KGE} = 0.9 * \text{KGE} + 0.1 * \text{noise}.$$

**Similarity.** The Cosine similarity is implemented as

$$1 - \text{Cosine distance}(\cdot, \cdot),$$

and the Euclidean similarity is implemented as

$$\frac{1}{1 + \text{Euclidean distance}(\cdot, \cdot)}.$$

**Linear probe.** We design a linear classifier to do link prediction for the KG. Note that we cannot implement the linear classifier on the large and sparse KG to do link prediction directly. To get meaningful results, we do negative sampling with sample number as 5. Then, we select to report the AUC (*Area Under the Curve*) score since other metrics cannot be differentiable under this condition. We randomly split the edge set of the KG into two even sets for training and test. To reduce variance, we repeat the experiment for 10 times.

**GCS.** We train our GCS model with input as noisy KGE and output as KGE. Note that here noisy KGE and KGE are in the same space, and the task is simpler compared to practical KI interpretation. Thus, we set the epoch number as 10, and use the reconstruction loss (i.e., mean absolute error) for efficiency. Other hyperparameters are set as the same as introduced in Appendix F.3.

<sup>15</sup><https://github.com/phanein/deepwalk>

## F.2. ERNIE and K-Adapter

**KI.** To ensure that the experiment settings are fair, we set hyperparameters as the default values. For **K-Adapter**, the code and hyperparameters for KI that we use are from the official projects<sup>16</sup> published by the authors (Wang et al., 2021a). The only two differences are that: we use PyTorch *float 32* instead of *float 16* since BERT and RoBERTa that we use are *float32*, and we use 4 NVIDIA Tesla V100 GPUs for KI training. For **ERNIE**, things are the same. All hyperparameters for KI are set as their default values<sup>17</sup>. Similarly, *float 16* of PyTorch is changed to *float 32*, and we do the integration with 4 NVIDIA Tesla V100 GPUs. Note that the dataset that ERNIE used for KI is Wikipedia, since the code is to fetch latest version of it, the data that we use could be slightly different. Therefore, for both ERNIE and K-Adapter, to ensure the fairness, we reproduce their KI, and report the results of reproduced models instead of results provided in their papers.

**Finetuning.** As for the downstream tasks, all the hyperparameters are consistent with the official project: either they are given in the project or in the README. In the same way, *float 32* and 4 NVIDIA Tesla V100 GPUs are chosen to make sure that the comparison is fair. Note that for K-Adapter and ERNIE, the best performance for different datasets is achieved in different settings. For example, the best performance for K-Adapter on the OpenEntity dataset is achieved with single GPU, but on the FIGER dataset is achieved with four GPUs. Since we focus on the relative performance instead of the best one, we run finetuning on 4 NVIDIA Tesla V100 GPUs for all downstream tasks and all LMs (as well as BERT and RoBERTa).

**Table 5:** Statistics of T-REx-rc and Wikidata

Datasets	Statistics	# of entities	# of triples	# of aligned sentences	# of entities (optimization)	# of triples (optimization)
T-REx-rc		781,275	1,282,504	5,565,478	-	-
Wikidata		3,275,534	12,849,311	-	1,344,393	3,240,272

The datasets that K-Adapter and ERNIE use are T-REx-rc and Wikidata, some statistics of them are given in Table 5.

## F.3. GCS

In this section, we introduce details of implementing GCS. In practice, GCS is composed of 3 layers: bijective MLP layer, graph convolutional layer, and another bijective MLP layer. As for bijective MLP layers, since weight matrices in them are square matrices, the dimension would remain unchanged: 768 for ERNIE and 1024 for K-Adapter. The nonlinear activation functions are set as ELU( $\cdot$ ) function, which is also bijective. The learning rate is set as  $1e^{-3}$ , and the dropout rate of the two MLP layers is 0.2.

Regarding the graph attention, to make sure interpretation results are stable, we apply multi-head attention mechanism, where the number of attention head is set as 8. Entity representations are first embedded into a space with the dimension as 64. Then, the embedded representations are used to calculate the attention coefficients. Note that since the purpose is to interpret and analyze the KI process, we do not split datasets for KI. Considering that GCS model is very simple for large KGs, overfitting is unlikely to happen. Thus, we optimize GCS for the whole datasets. Specifically, for K-Adapter, the whole KG is used for optimization, and results are used for interpretation. And for ERNIE, since the KG is very large, we sample a small subgraph with 1, 344, 393 entities and 3, 240, 272 triples for optimization (see Table 5), and then implement the optimized GCS on the whole KG for interpretation.

The objective function of training GCS can be reconstruction loss minimization or MI maximization. In this paper, except the synthetic experiment, we all select MI maximization as the objective. For reconstruction loss minimization, we use the mean absolute error (MAE) between our GCS outputs and entity representations of the knowledge-enhanced LMs. Regarding the MI maximization, we define the objective function by maximizing the MI as in Equation 4.

We optimize MI equation 4 by maximizing the compression lemma lower bound (Banerjee, 2006) as in Belghazi et al. (2018). The inputs of GCS are  $\mathbf{X}$ , and let the output be denoted by  $\mathbf{Z}$ . We can regard  $\mathbf{Z}$  and  $\mathbf{H}$  as empirical samples of random variables  $\mathbf{z}$  and  $\mathbf{h}$ . Thus, we have:

$$\text{MI}(\mathbf{z}; \mathbf{h}) \geq \sup_{T \in \mathcal{F}} \mathbb{E}_{\mathbb{P}_{\mathbf{z}\mathbf{h}}} [T] - \log(\mathbb{E}_{\mathbb{P}_{\mathbf{z}} \otimes \mathbb{P}_{\mathbf{h}}} [e^T]). \quad (12)$$

Here,  $\mathcal{F}$  can be any class of functions  $T : \Omega \rightarrow \mathbb{R}$  satisfying certain integrability constraints (Belghazi et al., 2018).  $\mathbb{P}_{\mathbf{z}\mathbf{h}}$

<sup>16</sup><https://github.com/microsoft/K-Adapter>

<sup>17</sup><https://github.com/thunlp/ERNIE>

represents the joint distribution of  $\mathbf{z}$  and  $\mathbf{h}$ , and  $\mathbb{P}_{\mathbf{z}} \otimes \mathbb{P}_{\mathbf{h}}$  represents the product of their marginal distributions. In practice, we let  $\mathcal{F} = \{T_{\theta_2}\}$  be the set of functions parameterized by a neural network, and optimize it by stochastic gradient descent. Then, the objective function can be rephrased as

$$\max_{\theta_1, \theta_2} \left( \mathbb{E}_{\mathbb{P}_{\mathbf{z}, \mathbf{h}}^{|\mathcal{V}|}} [T_{\theta_2}] - \log \left( \mathbb{E}_{\mathbb{P}_{\mathbf{z}}^{|\mathcal{V}|} \otimes \mathbb{P}_{\mathbf{h}}^{|\mathcal{V}|}} [e^{T_{\theta_2}}] \right) \right), \text{ where } \mathbf{z} = \text{GCS}_{\theta_1}(\mathbf{x}). \quad (13)$$

In equation 13,  $\mathbb{P}_{\mathbf{z}}^{|\mathcal{V}|}$  represents the empirical distribution of  $\mathbf{z}$ , i.e.,  $\mathcal{Z}$ . If the KG is very large, we can optimize the network by sampling a small subgraph of the KG. In practice, we simply add two MLPs layers to GCS for MI maximization. The added two MLP layers may not be bijective, where the dimension would be first reduced to 64, then to 1 for MI maximization. The nonlinear activation functions are all set as  $\text{ELU}(\cdot)$  function, which is also bijective.

For interpretation, we use the attention coefficients on edges and self-loops to analyze the KI in terms of triples and entities. Different from [Schlichtkrull et al. \(2020\)](#) that specially designs a discrete function to mask edges that are not important, we simply introduce a temperature hyperparameter  $t$  and set it as  $t = 0.1$  to make the attention coefficient distribution hard<sup>18</sup>. Thus, knowledge can be well clustered into learned and unlearned.

## G. Additional Statistics

**Table 6:** Drop statistics for the Integration Experiment.

Datasets	Statistics		
	Percentage of integrated entities	Percentage of integrated triples	# of aligned sentences/entity embeddings (integrated knowledge)
T-REx-rc	-	28.86%	561,687 out of 5,565,478
Wikidata	61.72%	-	2,240,260 out of 3,275,534

**Table 7:** Performance change of K-Adapter and ERNIE on the OpenEntity dataset with different test sets.

Model (Test set)	OpenEntity			
	Left test set	P	R	$\Delta\text{F1-Micro}$
K-Adapter (w/o IE)	37.44%	- 0.33	- 0.37	- 0.35
K-Adapter (w/o UE)	64.46%	- 0.18	+ 1.12	+ 0.47
ERNIE (w/o IE)	27.28%	- 18.20	- 25.14	- 22.67
ERNIE (w/o UE)	66.87%	- 0.31	+ 3.08	+ 1.57

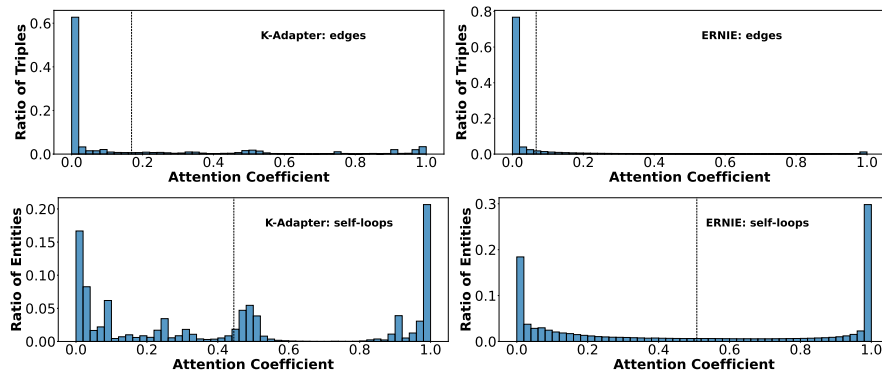


**Figure 8:** The attention coefficient distributions of edges and self-loops for K-Adapter and ERNIE. The histogram shows the empirical distributions (i.e., frequency), and the blue curves are the Gaussian kernel density estimate. The black dashed vertical lines indicate the average values.

Figure 8 presents the empirical distributions of attention coefficients for K-Adapter and ERNIE. The above two subfigures show distributions on edges, interpreting the KI from triples. While the bottom two subfigures show distributions of

<sup>18</sup>Note that the principle of hyperparameter selection is to maximize the MI, i.e., objective function. Users may select appropriate hyperparameters depending on the situation.

self-loops, illustrating the KI from entities. We can find that most knowledge triples are not integrated well for both K-Adapter and ERNIE (i.e.,  $a_{i,j} < 0.1$ ), while K-Adapter performs slightly better. When it comes to entity-wise integration, in general, entity knowledge is also not integrated well. We find that both CR (i.e.,  $a_{i,i} > 0.9$ ) and CF (i.e.,  $a_{i,i} < 0.1$ ) happens for many entities, especially for ERNIE. K-Adapter outperforms ERNIE since some entities are integrated well (i.e.,  $0.4 < a_{i,i} < 0.6$ ).

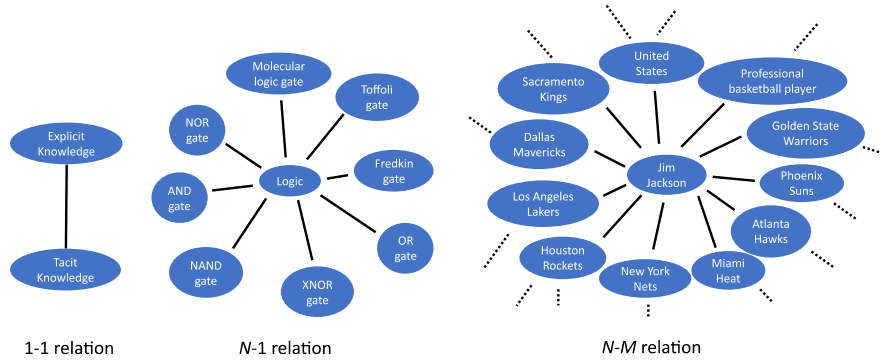


**Figure 9:** An example of different relations. The black solid lines are relations. We can find that nodes connect to multiple neighbors (e.g., "Logic") are more common than those leaf node (e.g., "OR gate").

**Table 8:** Analysis of KI interpretation results for K-Adapter and ERNIE in terms of different types of relations (topology feature). The percentages of integrated entities/triples, as well as of CR and CF entities for each type of relations are presented.

Statistics \ Model	K-Adapter on T-REx-rc			
	1 - 1 relation	N - 1 relation	N - M relation	Total
# of triples	21,690	813,674	1,729,644	2,565,008
Integrated triple percentage	58.89%	38.39%	24.00%	28.86%
# of connected entities	21,690	406,837	352,748	781,275
CR entity percentage	41.11%	31.72%	26.02%	29.41%
CF entity percentage	26.40%	30.29%	40.89%	34.97%
Statistics \ Model	ERNIE on Wikidata			
	1 - 1 relation	N - 1 relation	N - M relation	Total
# of connected entities	1,799	529,186	2,744,549	3,275,534
Integrated entity percentage	70.65%	42.86%	73.33%	68.39%
CR entity percentage	29.41%	56.07%	26.67%	38.28%
CF entity percentage	23.18%	8.65%	37.10%	32.49%

**Table 9:** The number of aligned sentences for relations.

Relation label \ Statistics	# of triples
Place of birth	134,976
Part of	134,999
Date of death	135,190
Date of birth	135,169
Located in the administrative territorial entity	135,055
Country	135,147
Total	5,565,478

## H. Additional Experiment

### H.1. Synthetic Experiment

In our first experiment, we simulate a synthetic KI processes where different amounts of knowledge is integrated into a LM, and test whether GCS can interpret it correctly.

**Setting.** We first use DeepWalk (Perozzi et al., 2014) to obtain entity embeddings (i.e., KG embeddings) of the KG that is

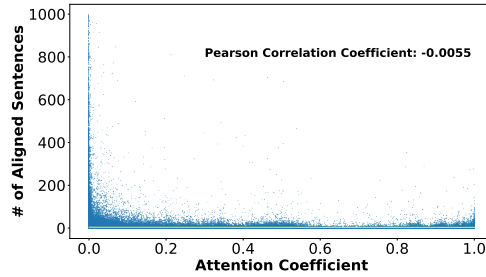


**Figure 10:** The correlation between the attention coefficient of the knowledge triple and its aligned sentence number for T-REx-rc dataset.

used for KI. We regard KG embeddings as the entity representations of knowledge-enhanced LMs, and we add Gaussian noise with different noise ratios on KG embeddings and regard it as the entity representations of vanilla LMs. The KG embeddings can be regarded as entity representations that contain almost all (i.e., 100%) information of the KG, and noisy KG embedding contain some (<100%) information of the KG. As noise ratio increases, it means that more knowledge is integrated in the LM. The synthetic KI process thus can be regarded as integrating factual knowledge from 50% to 100%. Then, we use GCS to interpret synthetic KI processes from vanilla LMs to knowledge-enhanced LMs.

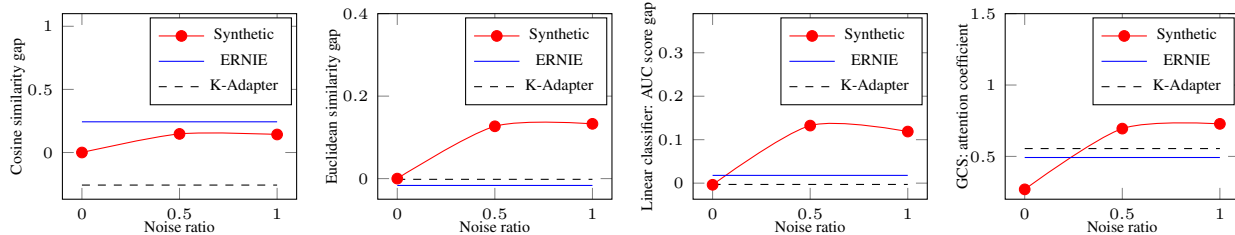


**Figure 11:** Interpretation results of how much knowledge is integrated based on different methods. Red lines with marks are interpretation results for synthetic KI processes. Blue solid lines and black dashed lines are the KI interpretation results of ERNIE and K-Adapter in practice.

**Baselines.** We select several baselines for comparison.

*Representation analysis.* In link prediction, intuitively, connected entities tend to have large similarity. Thus, for vanilla LMs and knowledge-enhanced LMs, we calculate the similarity (e.g., Cosine, Euclidean) between two connected entities to estimate how much knowledge about the triple is contained in the LM. Then, the similarity gap between vanilla LMs and knowledge-enhanced LMs can be used to interpret how much knowledge is integrated.

*Linear probe.* Similarly, we design a linear classifier (one linear layer) to do link prediction for the KG based on entity representations. The performance (i.e., AUC score) can be used to show how much knowledge is contained in the LM, and the gap between vanilla LMs and knowledge-enhanced LMs shows how much knowledge is integrated.

As for GCS, we use the mean value of self-loop attention coefficients to show how much knowledge is integrated: large values mean that little knowledge is integrated. For the convenience of observation, we report one minus its mean value in Figure 11. Implementation details are in Appendix F.1.

**Results.** Figure 11 shows the interpretation results. We observe the tendency of the red lines which show the interpretation results for synthetic KI processes. We find that except the linear classifier, other three methods provide correct trends: as noise ratio increases, the probe predicts that more knowledge is integrated. When we combine the practical interpretation results of ERNIE and K-Adapter, we can find that only GCS provides reasonable results: GCS predicts that these models integrate some factual knowledge. Other probes fail in interpretations: ERNIE and K-Adapter do not integrate any factual knowledge (linear classifier and Euclidean similarity), or they even forget learned factual knowledge (Cosine similarity).

## H.2. Linear Probe: Bias and Variance

We implement linear probe to interpret KI under the same settings as the synthetic experiment (Appendix H.1). Briefly, we train linear classifiers to do link prediction based on the entity label embedding for vanilla LM and knowledge-enhanced LM.

The intuition behind is that if the knowledge triple information is learned by LMs, it should be easy to use corresponding entity label representations to correctly predict the existence of relations. As for KI interpretation, we use the difference between prediction results of vanilla LM and knowledge-enhanced LM. Specifically, triples that are identified as learned in vanilla LM but unlearned in knowledge-enhanced LM are regarded as CF (catastrophically forgotten) knowledge, and triples that are identified as unlearned in vanilla LM but learned in knowledge-enhanced LM are regarded as integrated knowledge. Others are regarded as CR (catastrophically remembered) knowledge. Below we illustrate the reasons why linear probe is not suitable for KI interpretation.

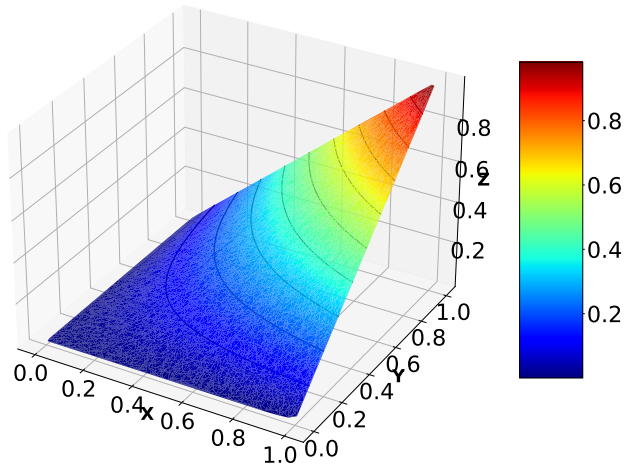


**Figure 12:** The accuracy of linear probe for KI and LMs. Here,  $x, y$  axes represents the probe accuracy for vanilla LM and knowledge-enhanced LM.  $z$  axis represents the probe accuracy for KI.

**Bias.** As we can see, KI integration is a process rather than a static LM to interpret. If we use probe models designed for LM to interpret KI, the error would grow exponentially. For example, the accuracy of probe results is 0.8 for vanilla LM, and 0.7 for knowledge-enhanced LM. Since only when the probe results for vanilla LM and knowledge-enhanced LM are both correct can we give correct interpretation for KI, the accuracy of interpretation results for KI is only  $0.8 \times 0.7 = 0.56$ . Figure 12 shows the relationships between the accuracy of KI and that of LMs. We can see that only when the linear probe model works extremely well ( $\text{Acc} > 0.9$ ) for LMs can it perform good for KI interpretation ( $\text{Acc} > 0.8$ ).

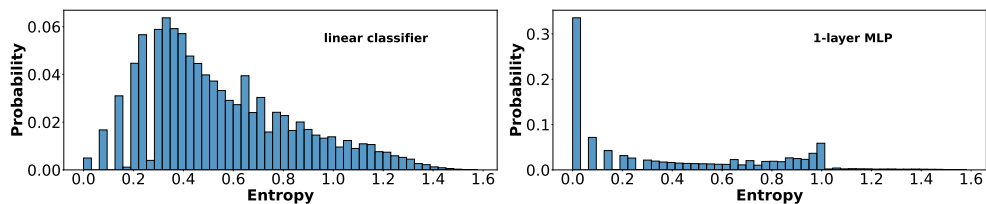


**Figure 13:** The entropy of probe results given by linear probe model (as well as MLP probe model) for KI interpretation.

**Variance.** We use 2-fold cross validation to interpret KI for all entities in KG. For the data split, we randomly split entities into two even sets. We repeat the experiment for 100 times, and check for the KI interpretation results for all entities. There are three types of interpretation results for each entity: CR, CF, and Integrated entities. We use its entropy to show the faith of KI interpretation results. For example, if the interpretation results for one entity is  $\{CR : 15, CF : 70, Integrated : 15\}$ , the entropy is 1.18. From Figure 13, we can find that for linear classifier, less than 10% entities are assigned with assured interpretation results. Most entities are assigned with diverse results (i.e., sometimes they are probed as CR entities, and sometimes they are probe as CF entities.) for different data split. Even if 1-layer MLP model could provide more consistent probe results, it is not suitable for probing since powerful neural models may learn the representations instead of probing it.

**Table 10:** The interpretation of KI, CR, and CF for K-Adapter in terms of relations and entities. We list 3 typical relations: CR happens to most connected entities; CF happens to most connected entities; and KI, CR, CF happens equally to connected entities. And we list 5 correspondingly aligned sentences. The Google Ngram of entities are reported to show the popularity of entities.

Relation label	Ratio of triples connected to CR entities	Ratio of triples connected to CF entities	Ratio of triples connected to WL entities	# of aligned sentences
KI of Entities (Google Ngrams)	Examples			
Copyright license CR, $(4.95, 2.47) \times 10^{-7}$	85.09%	14.61%	0.16%	4,400
Office held by head of government CF, $(0.91, 1.33) \times 10^{-2}$	0.46%	99.54%	0.00%	14,315
Opposite of CR, $(1.18, 1.77) \times 10^{-4}$ CF, $(3.67, 5.60) \times 10^{-2}$ WL, $(6.83, 2.46) \times 10^{-4}$	26.30%	41.87%	28.62%	11,577

### H.3. Case Study

**Knowledge of different entities (sorted by their popularity) has different CR and CF ratios (case study).** Table 10 reports the KI for K-Adapter in terms of entities<sup>19</sup>. We select three relations  $\{\text{“Copyright license”}, \text{“Office held by head of government”}, \text{“Opposite of”}\}$ . CR happens to most connected entities for relation “Copyright license”. CF happens to most connected entities for relation “Office held by head of government”. Some connected entities are learned well for relation “Opposite of”. We list 5 aligned sentences for the three relations, and report the Google Ngrams (year 2019)<sup>20</sup> of entities to show their popularity. We find that CF often happens to entities with large Google Ngrams such as “left” and “President”. And CR often happens to entities with small Google Ngrams. Well-learned entities are also not very popular.

### H.4. Relation Distribution

There are multiple features attached on edges in the KG. Here, we simply illustrate that existing graph neural networks cannot handle the relation label well since there are some difficulties.

- **The number of relations is large.** The KG used in ERNIE has 594 distinct relations and the KG used in K-Adapter has 410 distinct relations. In RGCN (Schlichtkrull et al., 2018), they use different sets of parameters for different relations when doing neighborhood aggregation. It is hard to implement hundreds or thousands of sets of parameters to analyze KI. Besides, in our GCS model, we have to include attention mechanism for interpretation. The number of parameters for attention mechanism is also hard to be scaled to 400 – 500 times. Even if we can address this technical issue, using such as heavy probe model for analysis is also unrealistic.
- **The distribution of relation number is highly imbalanced.** As shown in Figure 14, we can see that the distribution (i.e., PDF) of relations is very imbalanced. For ERNIE, 10% relations account for 93% edges, and 5 relations (around 1%) account for 50% edges. For K-Adapter, 10% relations account for 78% edges, and 5 relations (around 1%) account for 29% edges. Simply treating each relation by one set of parameters in interpretation could provide unreliable results.

Besides above mentioned points, other factors such as multi-edges (i.e., two entities may have multiple distinct relations between them) are also challenging to tackle. In summary, to support relation information in our GCS model, users should carefully select powerful graph filters (i.e., graph neural network models) based on the specific scenario. We would like to leave the exploration for future work.

<sup>19</sup>Entities with  $0.4 < a_{i,i} < 0.6$  on self-loops as well-learned (WL) entities.

<sup>20</sup><https://books.google.com/ngrams>

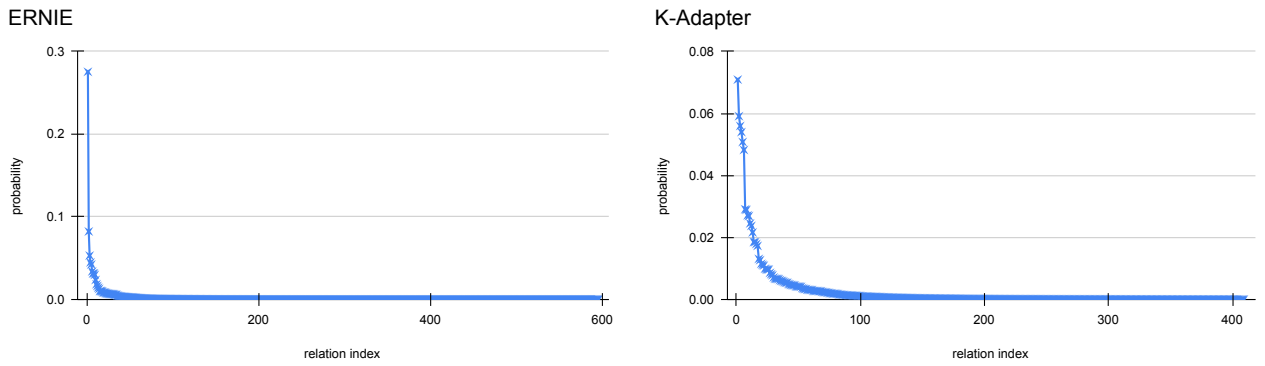


**Figure 14:** The distribution of relation number for KGs used in ERNIE and K-Adapter.